2013

Radial Diffusion of Florescein Molecules (376 DA) in Canine Bone Tissue

Daniel O'conor
Cleveland State University

RADIAL DIFFUSION OF FLUORESCEIN MOLECULES (376 DA) IN CANINE BONE TISSUE

DANIEL O'CONOR

Bachelors of Science Biology

The Ohio State University

June 2010

Submitted in partial fulfillment of requirements for the degree of

MASTER OF SCIENCE IN BIOMEDICAL ENGINEERING

at

CLEVELAND STATE UNIVERSITY

December 2013

We hereby approve this thesis of

Daniel P. O'Conor

Candidate for the Master of Science in Biomedical Engineering degree for the

Department of Chemical and Biomedical Engineering

and the CLEVELAND STATE UNIVERSITY

College of Graduate Studies

_____

Thesis Chairperson, Dr. Joanne M. Belovich

_____

Department & Date

_____

Thesis Committee Member, Dr. Surendra N. Tewari

_____

Department & Date

_____

Thesis Committee Member Dr. Ronald J. Midura

_____

Department & Date

Student's Date of Defense: December 4, 2013

This thesis is dedicated to science… you're welcome.

ACKNOWLEDGEMENTS

First and foremost I'd like to acknowledge my thesis committee. Without their help and support I would have truly been lost. I would like to thank Dr. Belovich for always being available and ready to answer any questions I had and nudge me in the right direction. Her patience and understanding was greatly appreciated as I transitioned from biologist to engineer. I would like to thank Dr. Tewari, whose knowledge and experience in research helped me appreciate attention to details and always encouraged me to take a step back and look at problems from different perspectives. Dr. Midura at the Cleveland Clinic helped me understand all of the in depth knowledge of the biochemical aspects of this research and made this research possible. And finally, Dr. Androjna, who was always willing to take time out of her busy day to help me in the lab with any problems I came across.

Outside of my thesis committee, I'd like to thank the algae and bone research groups in the biochemical engineering labs at Cleveland State University for always helping out and making me laugh when things got hard. I would also like to acknowledge the entire staff at Cleveland State University, especially Becky Laird for all of her help and hard work in the Department of Chemical and Biomedical Engineering.

RADIAL DIFFUSION OF A 376 Da MOLECULE IN CANINE BONE TISSUE

DANIEL O'CONOR

ABSTRACT

The ability to maintain homeostasis in any biological tissue is extremely important and accomplished via the transport of vital nutrients into and removal of waste out of the tissue. The understanding of transport processes in tissue can lead to the ability to design and manufacture new medications, viable replacement tissues, and prosthetic implants to replace diseased or degraded biological tissue. Specifically, bone tissue, which is a heterogeneous tissue, tends to degrade as one ages to the point that the tissue easily fractures. A custom two-chamber diffusion cell was used to measure the effective diffusion coefficient *in vitro* of 376 Da fluorescein sodium salt through the canine tibia. The system was maintained at 37°C and various concentrations of fluorescein were placed in the donor chamber. Samples were taken from the receiver chamber every 24 hours over a period of 7-10 days, and analyzed by a fluorescence spectrophotometer. The model equation for quasi-steady state transport in *Truskey et al.*[11] was used to find the effective diffusivity. It was found that the one dimensional radial diffusivity through canine bone tissue was $1.57\text{x}10^{-7} \pm 3.17\text{x}10^{-8}$ cm^2/s at 0.3 μM, $6.74\text{x}10^{-8} \pm 1.00\text{x}10^{-8}$ cm^2/s at 30 μM, and $1.36\text{x}10^{-8} \pm 1.93\text{x}10^{-9}$ cm^2/s at 300 μM. The average distance between a Haversian canal and an osteocyte is 100 μm[44] meaning it will take fluorescein around 5, 12, and 61 minutes at 0.3, 30, and 300 μM respectively to traverse the distance in unloaded conditions. This is a good indicator for the diffusion time of a key nutrient in bone, Vitamin D, which is similar in size (384 Da) and structure. It was also found that as the initial donor concentration increases, the diffusion coefficient decreases.

TABLE OF CONTENTS

Page

LIST OF FIGURES

Page

LIST OF TABLES

Page

CHAPTER I

INTRODUCTION

The prevalence of bone disease in the United States is relatively high, especially in people over the age of 50, and is only going to increase in the coming years as the population grows older. Osteoporosis and low bone mass are the most commonly diagnosed bone disorders with as many as 40 million people having or being at high risk of having bone disorders in the United States alone. That number is expected to rise significantly and by 2020, one in two Americans over the age of 50 is expected to have or be at risk to have a bone disorder[23]. Currently, there is plenty of research available on the structure and physiology of bone tissue and how it maintains homeostasis or is impaired by diseased states. With that being said, it is vital for researchers to fully understand the transport properties of essential nutrients inside of bone in order to create and manufacture pharmaceuticals to treat or prevent these bone disorders. This section

discusses prior research methods used to analyze the transport properties, specifically diffusion, of various molecules in bone tissue.

Bone is a remarkable material whose primary functions are to act as the central support system for the human body, serve as a mechanical basis for locomotion, and to protect the vital organs such as the brain, spinal cord, and heart. Bone is a complex and dynamic connective tissue that interacts with numerous surrounding tissues including vascular tissue, cartilage, nervous tissue, epithelium, adipose tissue, and other connective tissues[1]. There are two types of bone in the human body. The solid shell is known as cortical bone and the spongy bone is known as trabecular bone[2]. All bone is made of a matrix of organic and inorganic parts. The inorganic part has principal components of water, and a calcium and phosphorus salt known as hydroxyapetite. The organic components consist of collagen, non-collagenous proteins, osteocytes, and various growth factors. There are also trace amounts of magnesium, sodium, and bicarbonate within the bone matrix[1].

Bone is a dynamic tissue, it is continuously breaking itself down, rebuilding and remodeling in order to stay healthy. A constant supply of nutrients and removal of wastes is crucial and must be sustained in order to encourage healthy bone tissue in the body. Because of the dynamic nature of bone, it is important to quantify these rates of nutrient and waste exchange within the bone tissue. Knowledge of the transport rates of vital nutrients in bone can improve one's ability to design drugs and medications that would target specific areas of bone tissue. This information can also improve the understanding of bone physiology and the healing process of bone tissue after injuries like breaks and sprains by quantifying the rates at which damaged or necrotic tissue is purged and

replaced. The healing process is dependent upon the rate at which the body can exchange nutrients and signaling factors and remove waste products. For that reason, being able to establish the rate of transport in bone tissue could prove beneficial in aiding medical researchers develop novel solutions to diseased states in bone tissue.

Diffusion is one of the main means of nutrient transport in bone tissue. Although diffusion in bone tissue has been previously studied, there are some uncertainties with the recorded rates due to the molecules used and the complexity of the human system. The intention of this paper is to accurately quantify the effective diffusion coefficient of a small molecule (376 Da) in the radial direction through bone tissue. Transport in the radial direction was chosen for two reasons. First, most previous research is in the axial direction, with little research in the radial direction. Second, transport rates in the radial direction are expected to be much slower than that in the axial direction where vascular transport dominates.

The effective diffusion coefficient of fluorescein sodium salt through the cortical bone of the canine tibia was measured in the absence of a mechanical force. The specific aims of this thesis are to establish the rate at which a small molecule diffuses through bone tissue at various concentrations and to determine if the effective diffusion coefficient is a function of the species concentration.

A standard two-chamber diffusion cell was used with a tissue sample approximately 470 um thick placed between the chambers. Concentrations were quantified using a fluorescence spectrophotometer. A quasi-steady state transport model was applied to quantify the rate at which the molecule diffused through the bone tissue in the radial direction in one dimension. The results allow one to estimate the transport rates

of similar molecules *in vivo* in the absence of mechanical loading, and provide a baseline measurement for quantifying the effect of mechanical loading on transport.

CHAPTER II

BACKGROUND

2.1 Bone Structure and Composition

2.1.1 Bone Architecture

Adult human bone tissue is a biocomposite material that is composed of approximately 67% mineral salts and 33% organic matrix. Its organic matrix components consist of 62% type I collagen and 26% minor collagens and non-collagenous proteins, 6% lipids and 6% complex carbohydrates[3,4]. On the larger scale, bone can be separated into two types: cortical bone and trabecular, also known as cancellous, bone (Figure 2.1). Each of the two types of bone has a different structure which influences its structure and function.

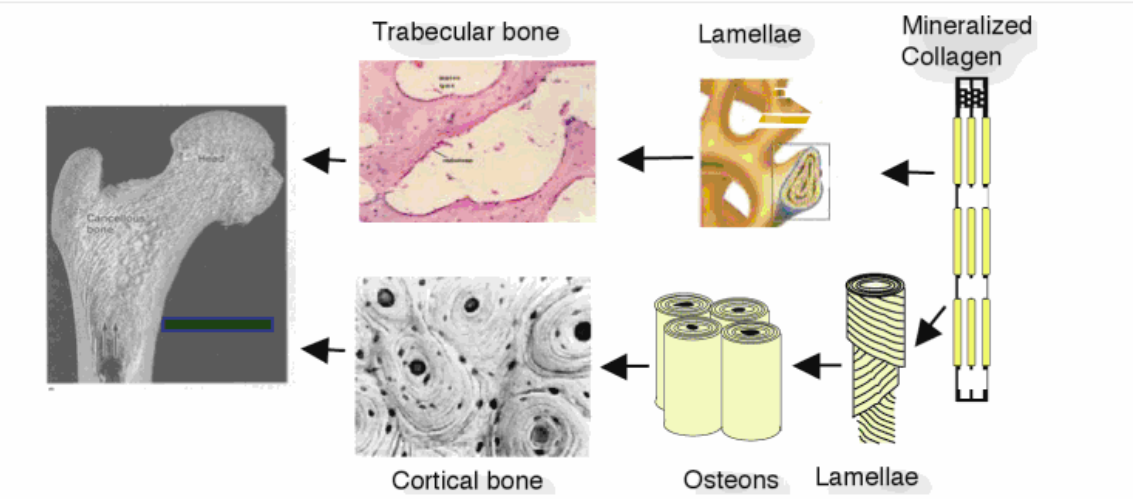

Figure 2.1 Cortical vs. Trabecular bone[5]

Trabecular bone is found inside the medullary cavities of long bone at its epiphyses and metaphyses. Trabecular bone has three main components: trabeculae, lacunae, and bone marrow with a 75%-95% porosity of its total volume[5]. Since trabecular bone has such a high porosity, diffusion is generally not limited and thus is not the focus of this study.

The focus of this study, cortical bone, is much denser than trabecular bone and has a porosity of only 5%-10% of its total volume[6]. Cortical bone accounts for nearly 80% of the total mass of the human skeleton yet remodels at 1/10th the rate of trabecular bone. Therefore cortical bone is a vital element in tissue engineered bone substitutes[6]. Given that cortical bone is the denser of the two types, it should be more diffusion limited. The structural features of cortical and trabecular bone are presented below in Figure 2.2.

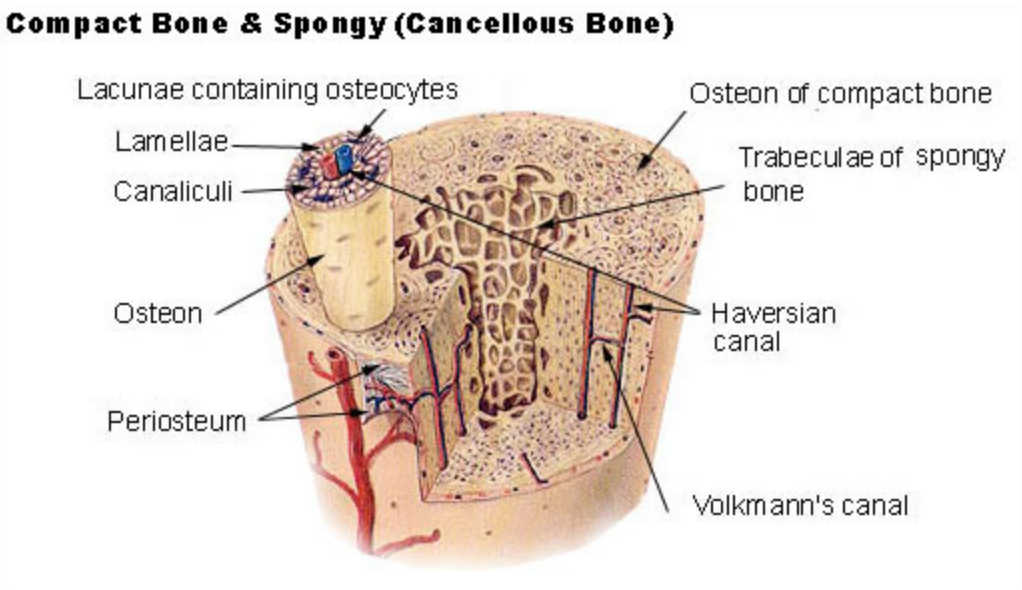

Figure 2.2 Structure of Cortical Bone[24]

Figure 2.2 shows a transversely sliced bone tissue which clearly displays the most important features needed for nutrient transport in bone tissue. The largest fundamental unit is the lamellar osteons, also known as the Haversian system. These osteons are roughly cylindrical in shape with an average size of 250 micrometers in diameter. The center of an osteon, called the Haversian canal, runs along the long axis of the bone and surrounds nervous tissue and blood vessels located in the center. Each osteon is separated by a boundary layer known as the cement line. Interstitial tissue, which is constantly being broken down and remodeled, surrounds the cement line. Small cavities called lacunae are where osteocytes are located and are constantly in communication with one another via tiny canals called canaliculi.

There are also much smaller structural components that are important in the radial transport of nutrients to bone tissue. These features run perpendicularly to the length of the bone and have a large role in radial diffusion. One such feature is the Volkmann's canals. These small canals connect the larger Haversian canals to one another and are

vital to this radial diffusion study. In addition, reabsorption cavities are temporary voids created by bone-removing cells in the beginning phase of bone remodeling. Canaliculi are a multi-directional pore system by which molecules could diffuse through, yet are a very minor means of diffusion since they only contribute around 10% of the overall 5%-10% porosity in dense cortical bone[7,10]. One important fact to keep in mind is that all of these canals and their porous network do not run at exact right angles to each other nor are they perfectly parallel or perpendicular to the long axis of the bone[11]. The canals of the vascular network comprise a mixture of orientations, often forming an oblique angle with the surface of the bone. All of these canals and cavities that form the porous network in bone work to maintain homeostasis by allowing for the exchange of vital fluids, nutrients, and waste products[8,9,10].

2.1.2 Porosity and Connectivity of Bone Tissue

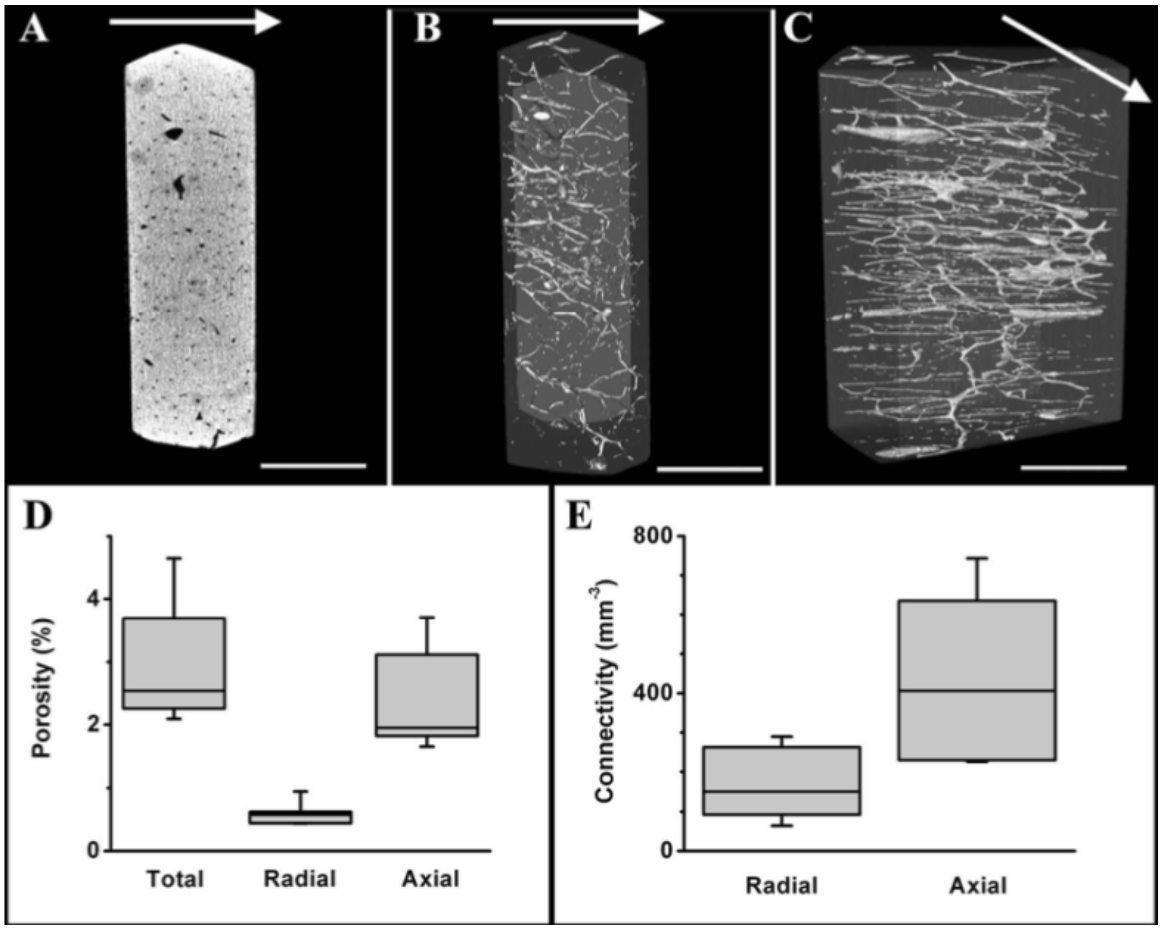

Figure 2.3 (A) Representative 3D micro-CT scanning image. (B) Inverted 3D micro-CT image in the radial direction. (C) Inverted 3D micro-CT image in the axial direction. (D) Graph of Porosity. (E) Graph of Connectivity.[12,13]

Past studies have analyzed the internal structural properties of cortical bone using a Micro-CT scan to quantify the inner network of the bone tissue. The bone samples analyzed in *Wen et al*[13]. were taken from the same canine (Lot #07D-256) as the bone used in these diffusion trials. Using 3D micro-CT (figure 2.3), it was found that each bone wafer from the endosteal surface displayed numerous large pores of 50-100 um in width and intermediate-sized pores of 10-50 um in width. Imaging done on the opposing surface of the bone wafers showed no large pores, fewer intermediate pores, but numerous small pores ranging from 1-5 um in width[10,12,13]. Observing that there are pores

on both ends of the sample, they investigated whether the pores connected across the bone using 3-D Micro-CT imaging at 3 μm resolution. The results of the imaging revealed that the pores were indeed interconnected both radially and axially. Using the results from the 3-D Micro-CT the researchers calculated the total porosity of their samples as 2.95 +/- 0.91%. The radial porosity of the sample was 0.60 +/- 0.17%, and the axial porosity was 2.36 +/- 0.71%[12,13]. Calculations revealed the connectivity density for radial connectivity of 175 +/- 87 mm^3 and axial connectivity of 438 +/- 204 mm^3 [12,13].

2.2 Selection of Animal Model

Since this study is based on diffusion through cortical bone tissue, the growth and biochemistry of the sample is not as important as the actual physiological structure of the bone tissue when compared to human bone tissue. In humans, bone structure is dependent on various factors including age, gender, and anatomic location[2]. Many animal models have been developed and proposed for clinical trials; however, each has their own uses and limitations in the study of human bone tissue engineering. A lot of research has been performed on the differences in bone structure, density, and overall quality among various species including dogs, sheep, chickens, cows, and pigs. Based on a review of the current literature, it was decided that canine bone tissue was the best overall model for cortical bone diffusion trials. Bone composition and architecture, most importantly density and porosity, were most similar between humans and canines[14,15]. Due to previous studies and data already gathered, we contend that our canine diffusion model is translatable to human bone tissue.

2.3 Layer of Bone Tissue Studied

Figure 2.4 shows the location of the harvested bone samples used in this study.

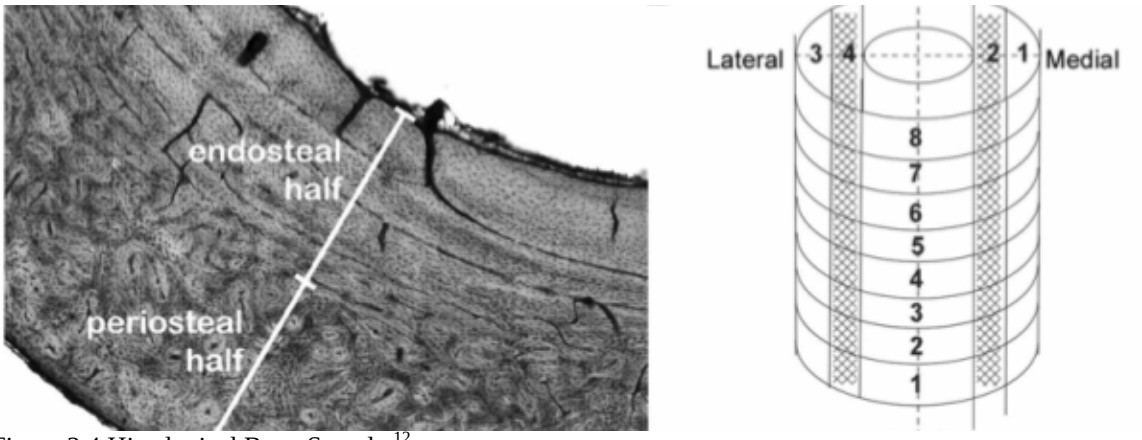

Figure 2.4 Histological Bone Sample.[12]

The right side is a sketch of the pre-cut cortical bone sample with the shaded area representing the region of bone used in the diffusion trials. The left image is a magnified histological slice of bone showing the periosteal and endosteal regions of cortical bone. This image clearly displays the different organizational networks of the Volkmann's' canals in the periosteal half compared to the endosteal half. Many papers have investigated these networks and have found more success in measuring radial permeability in the endosteal halves than in the periosteal halves[14,16,17]. Specifically, it was commonly found that the fluid movement through the bone samples in the endosteal to periosteal direction was so small that they were below the limits of detection with no numbers being reported. Studies found that when ~3.6% of the bone thickness was removed from the periosteal surface, fluid would pass through the bone sample. For this particular study, we removed ~0.5-1.0 mm of bone from the periosteal surface using a slow-speed bone saw. These findings led to us using bone samples from the endosteal region of the canine cortical bone for all diffusion trials.

2.4 Diffusion in Bone Tissue

2.4.1 Theoretical Overview

The transport of molecules in a fluid can typically be described via two methods: diffusion and convection. Diffusion is defined as random motion of molecules that arises from thermal energy transferred by molecular collisions[11]. Diffusion is also known as Brownian motion, named after the scientist Robert Brown who originally developed the concept. Convection is the mechanism by which transport results from the bulk motion of fluids[18]. Each of these mechanisms independently and concurrently influences the movement of mass and its momentum in biological systems. Convection in this study is absent, the primary focus being diffusion.

A molecule in the gas or liquid phase will have random interactions with its surrounding environment. Several factors influence the diffusion of molecules such as the size and shape of the molecule, temperature, and fluid viscosity. Although diffusion is defined as random motion of the molecules, there is always a net motion or direction in which the diffusion occurs. Movement is primarily from areas of high concentration to areas of low concentration. The rate at which a molecule flows per unit area is known as flux, and diffusion flux is proportional to the gradient of the solute concentration[18]. The idea of flux was first quantified by scientist Adolph Fick and is now known as Fick's Law[18]:

$$J = -D\frac{dC}{dx}$$

The variable J is the diffusion flux and D is the diffusion coefficient, which is a function of both pressure and temperature. For this study, quasi-steady state transport conditions

were applied since the timescale by which the surface concentration changes is much slower than the timescale for diffusion across the bone sample[18]. A simple approximation is derived (see Methods section) for which it can be assumed that the diffusion in the sample is much faster than the diffusion that leads to the change in concentrations at the boundaries. If this approximation is satisfied, steady-state transport across the membrane can be assumed.

2.4.2 Role in Biological Tissue

Homeostasis of the human body is extremely important and the diffusion of essential molecules plays a vital role in maintaining homeostasis in all living organisms[19]. The rate at which a molecule diffuses is a function of the properties of the specific molecule, the direction of transport, and the composition of the material in which the diffusion is occurring. Bone tissue, which is a heterogeneous structure, is formed by the accumulation and assembly of cells and organic matrix material in the extracellular space[20]. The heterogeneous composition of bone tissue can have a huge influence on the local rates of molecular transport throughout the tissue affecting the overall rate of diffusion. For this experiment the focus was diffusion through a thinly sliced sample of bone tissue with the ultimate goal of creating a synthetic construct with identical diffusive properties as native human bone tissue, since bone grafts and replacements largely depend on diffusion of molecules for growth and repair.

The health of bone tissue is largely dependent upon an efficient mode of transport of vital molecules between the blood supply and cells embedded within the bone tissue[21]. Currently there is significant research that shows a pronounced and rapid flow of

molecules through the extravascular spaces in bone tissue[22]. Most *in vivo* experiments focus on injecting large molecules directly into the bone tissue of various animal models and monitoring the movement throughout the various pathways in cortical bone. These experiments are important, however they do not differentiate between radial and axial diffusion. In fact, in most cases, researchers primarily focus on axial diffusion. Regardless, it is apparent that diffusion is one of the primary mechanisms of transport within bone tissue. This experiment focuses on diffusion in the radial direction in bone due to the relative lack of data and literature in this particular area.

In summary, nutrient transport across bone tissue is imperative for cell viability as well as overall tissue health. The ability of fluids and molecules to transport through porous material is an inherent property of bone tissue. Overall, this ability is affected by the tissue architecture and porosity, biochemistry of the matrix, and the pericellular fluid properties[22]. By initially quantifying a baseline value for the diffusion coefficient *in vitro*, following experiments can interpret effects of external factors such as mechanical, chemical, and/or electrical factors on the baseline diffusion coefficient. With a better understanding of diffusion within the bone tissue, researchers should be able to better design pharmaceuticals, bone tissue scaffolds, and prosthetic implants.

2.5 Relevant Studies on Diffusion

Diffusive properties of bone tissue in the early stages focused more towards pore size than actual transport properties. Knowing that bone tissue is not uniformly porous, the idea was to find a biocompatible substance that had a similar porosity to bone tissue. These studies found the minimum pore size in ceramic scaffolds for significant growth of

natural bone ranged from 75-100 μm[25]. Once these numbers were established, researchers turned their attention to computational modeling of the fluid dynamics in bone. A qualitative study by *Dillamen et al*. conducted in 1991 computationally looked at the time required for nutrients to diffuse within rat and chicken bones[21]. Using large molecules such as ferritin (440 kDa) and horseradish peroxidase (44 kDa), the researchers noticed that after injection these molecules had been localized throughout the osteocytic lacunae and canaliculi of cortical bone in both the rat and chicken bone samples. Although no numbers were reported, the researchers observed bulk flow in even the densest portions of bone. This research provided evidence that transport occurs in even the densest areas of bone tissue, providing the foundation for future diffusion studies.

The next step after bone characterization and computational modeling was to look at qualitative non-loaded bone transport studies. A study performed by *Knothe-Tate et al*. hypothesized that diffusion alone cannot be responsible for molecular transport in bone tissue[29]. To test this, the group used procion red dye (615 Da) and paralyzed rats to study the transport of the molecules into the bone tissue. These tests consisted of long term and short term *in vivo* studies on rat bones, looking at cross sectional cuts of the bones under a fluorescent microscope. The results led the group to the conclusion that diffusion alone could not be an efficient means of transport of larger molecules. They argued that connective tissue transport by a load induced fluid flow could be the answer to transporting larger sized nutrients in bone tissue[29,30]. *Knothe-Tate et al.* used this conclusion to move on to more quantitative studies. Although non-loaded research on transport rates helps to present a control for how molecules transport in bone tissue, they are not as physiologically relevant as load-induced transport studies.

The most logical next step in studying molecular transport in bone tissue was to study the effect of mechanical loading on the transport rates in bone. Another study by *Knothe-Tate et al.* looked first at the qualitative aspect of loaded diffusion before moving on to the quantitative aspect. They showed that diffusion was indeed occurring under loaded conditions and possibly at a higher rate than unloaded conditions. The study hypothesized that load-induced fluid flow augments the transport of important molecules which help regulate cellular activity associated with processes of functional adaptation and remodeling[28]. The study was performed *in vivo* within the tibia of a rat. The experimental set-up consisted of a 4-point bending apparatus applying specific mechanical loads to the bone sample. Using a red tracer molecule, they showed that mechanical loading significantly improves molecular transport in the diffusion limited matrix of cortical bone[28]. This was only a qualitative study as again, no numbers were reported and advised for further studies. One must be careful with this data however, as rat bone lacks in quantity of osteons and has low Haversian remodeling, which is different from native human bone tissue[33].

Knothe-Tate et al. continued their research on transport rates in bone tissue with another qualitative study. The study again focused on mechanically loaded bone, but this time used a bone sample from a sheep. The bone was compressed in short cycles; every 2, 4, 8, 16 minutes, and was compared to an unloaded bone control sample. The research group used procion red dye (615 Da) along with the FRAP technique (fluorescence recovery after photobleaching) to gather data, but again did not report any numerical values for diffusion. The results pointed to relatively higher transport rate in the mid-diaphysis of the cortex of the loaded bone compared to the unloaded control sample[15].

Some drawbacks of the experiment were that the bone was screwed in to the apparatus and tension/compression was applied to the bone laterally. Also, they did not differentiate between radial and axial flow.

To expand on the FRAP technique mentioned above, it is important to look at the research group who developed it. *Wang et al.* developed this technique to quantitatively measure diffusivity in various biological tissues[27]. The FRAP technique begins by gathering images of the sample, saturated in fluorescent dye, using the laser scanning confocal microscope. Tissue level diffusion is measured by bleaching a region in the tissue consisting of a matrix, canaliculi, and lacunae and measuring the recovery of the fluorescent probes. This is measured by calculating the mean intensity of the bleached region within an image collected after bleaching. Thus, the technique focuses on transport between individual canaliculi within the dense tissue portion, and not across the entire tissue sample[27].

Once a technique to measure diffusion was established (FRAP), *Wang et al*[27]. shifted their focus to the molecule being transported. Their study used fluorescein sodium salt, the same molecule used in this thesis, to measure the diffusion values in bone. The group used the FRAP technique with a small alteration - the fluorescein sodium salt was injected into individual osteocytic lacunae and visualized *in situ* beneath the periosteal surface of cortical mouse bone at depths up to 50 micrometers with laser scanning confocal microscopy[28]. This study reported a numerical value for the diffusion coefficient of fluorescein sodium salt through a single canaliculi as 3.3×10^{-6} cm^2/s. The researchers noted that this value is 62% of its diffusion coefficient in water and is similar to coefficients of similarly sized molecules. Again, it should be pointed out that mouse/rat

bone tissue is not a physiologically similar to humans as other animal models[33]. Although this value is only for a single canaliculi and not an entire tissue, transport is not totally unimpeded. Canaliculi contain many twists and obstacles within such as charged ions and lipids. Given the biochemistry of lipids, they could have a considerable effect on transport rates of fluorescein sodium salt due to the salt's ability to capture and hold charged particles. Keep in mind that a canaliculi is just one pathway a molecule can follow in bone tissue, and in this thesis all radial pathways will be used in a bone slice.

The Knothe-Tate research group used the FRAP technique again in another one of their studies. They measured the diffusivity at the matrix-porosity level and found it to be 7.0×10^{-10} cm^2/s using a 300 Da dye[26]. This value is considered extremely low, bearing in mind the dense, inorganic nature of this portion of bone tissue. The research group then used a 3000 Da molecule in the axial direction of the bone sample and recorded a value of 3×10^{-10} cm^2/s diffusion rate. The end of their paper questioned the validity of this number for the 3000 Da molecule but did not expand upon it. They did however distinguish between radial and axial diffusion, which was new for this research group.

A group of researchers, *Lang et al*, reported diffusivity data using a method other than the FRAP technique[31]. This group of researchers used radioactively labeled glucose to measure the diffusion rates in a canine femur. The bone sample was placed in a specially designed diffusion chamber that allowed for loaded and non-loaded experiments to be performed on the sample. Concentration was measured by determining the number of radioactively labeled glucose molecules that had penetrated into the bone sample. They reported a value of the diffusion coefficient to be 3×10^{-9} cm^2/s. The experiment was repeated under non-loaded conditions and found no significant difference in the

value of the diffusion coefficient compared to the loaded experimental conditions[31]. The research group pointed out some of the design flaws of the experiment, mainly the use of a grinder to remove the peritoneal surface of the bone samples which could have blocked some pores and thrown off their mathematical model, which is dependent upon uniform surface porosity of the bone sample. Also, their concentration is in units of cpm/ml which is a radioactive counting technique of a molecule per milliliter. The researchers never give an initial molarity so it is difficult to extrapolate their data to a physiological benchmark.

A study carried out by *Fernandez-Seara et al.*[32] measured diffusivity in bone by using a combination of radio-nucleotides and NMR to calculate their values for the diffusion coefficient. They used radioactively labeled water, D_2O, and studied its transport across the mineralized matrix of bone using proton nuclear magnetic resonance spectroscopy and imaging to measure the diffusion fluxes of tissue water in cortical rabbit tibia. The researchers calculated the diffusion coefficient to be 7.8×10^{-7} cm^2/s at 40°C[32]. They made an important observation that diffusion rates were higher close to the endosteal and periosteal surfaces and decreasing towards the center of the cortex, which is the opposite of other reports[32]. Like mice and rats, rabbit bone also differs in structure from that of a human. Rabbit bone has vascular canals that run parallel to the long axis of the bone and the micro and macro structure is dissimilar to human bone[33].

An interesting aspect of the diffusive properties in bone is the effect of concentration on the rate of transport in porous media. It was observed in this thesis experiment that the concentration of FITC in PBS affected the rate at which it diffused in bone tissue with the relationship that as concentration of FITC in the donor cell increases,

the overall diffusion coefficient decreases. However, there is very limited amounts of literature on this finding, and none found using bone as the porous media. A research group, *Albro et al*, noticed this trend when studying fluorescein-conjugated dextran diffusion in agarose hydrogels under loaded conditions[34]. They then used FRAP to measure the diffusion coefficients at each concentration, ranging from 7 μM to 50 mM fluoescein-conjugated dextran in PBS. The research group found that the diffusion coefficient decreased as the dextran concentration increased. The results from their study demonstrated that for increasing solute concentration in the presence of a solid gel network, the dextran diffusivity exponentially decreases toward a value of zero. Although this study was not done in bone tissue, they believe the results are translatable for similar molecular weight solutes in other porous media.

In summary, there are limited amounts of literature on the transport rates of molecules in bone tissue and most of them provide immensely different values compared to each other. These differences in numbers can be attributed to the selection of the animal model and/or the technique used to measure diffusion. That is why most publications give the disclaimer that, "The literature reports on quantitative diffusion measurements in bone tissue are sparse[32]". The table below, Table 2.1, summarizes the diffusion coefficients and their experimental technique previously discussed in this section and compares them to the values of the fluorescein sodium salt molecule diffusion coefficient in water.

	Diffusion Coefficient cm^2/s	Description of area measured	Solute Used	Reference
Smallest	3×10^{-10}	FRAP method entire cortical bone	3000 Da dye	Patel and Knothe-Tate et al.[26]
	7×10^{-10}	FRAP method entire cortical bone	300 Da dye	Patel and Knothe-Tate et al[26]
	3×10^{-9}	Entire femur	Glucose (180 Da)	Lang et al.[31]
	3.28×10^{-8}	Fluorescent imaging cortical bone beam	Fluorescein (376 Da)	Gonzalez[40]
	1.27×10^{-7}	Fluorescent imaging cortical bone beam	Fluorescein (376 Da)	Farrell[39]
	8×10^{-7}	Cortical bone using radioactive markers	D_2O	Fernandez-Seara et al.[32]
	3.3×10^{-6}	FRAP methodology in a single canaliculi	Fluorescein (376 Da)	Wang et al.[27]
	7×10^{-6}	Diffusion in water only (no bone)	Glucose (180 Da)	Landolt-Bornstein et al.[37]
Largest	2.7×10^{-6}	Diffusion in PBS only (no bone)	Fluorescein (376 Da)	Periasamy et al.

Table 2.1 Summary of diffusion coefficients found in bone tissue and a comparison of known fluorescein sodium salt and glucose diffusion coefficients in water.

2.6 Fluorescence Spectrophotometer

A crucial aspect of this research is the use of a fluorescence spectrophotometer, or fluorometer. This instrument analyzes the fluorescence of a sample via a beam of light, in this case from a xenon lamp, which excites electrons in the sample and causes these electrons to emit light which is then measured by the fluorometer. For this experiment fluorescein, a sodium salt, was used. Fluorescein is water soluble and in solution it is a salt. The ionic and nonionic structure of fluorescein is shown in Figure 2.6. Its maximum excitation peak is in the blue-green spectrum at 494 nm and its maximum emission peak is in the green spectrum at 518 nm[35]. Fluorescein is known to have one of the brightest

low-molecular-weight fluorescent chromophores known, with a quantum efficiency of 0.9[35]. These tangible qualities make fluorescein an ideal choice for studying bone diffusion rates via fluorescence.

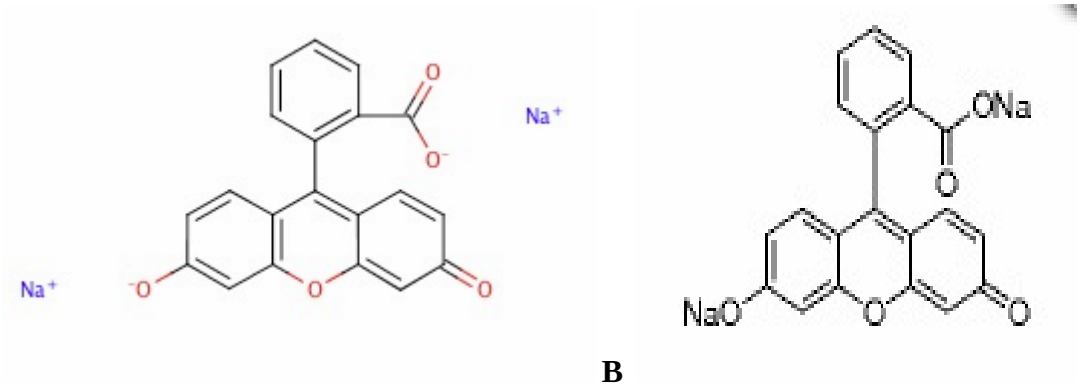

A **B**

Figure 2.5 (A) Fluorescein sodium salt in ionic form. (B) In non-ionic form.[39]

2.7 Molecules with Structures Similar to Fluorescein Found in Bone Tissue

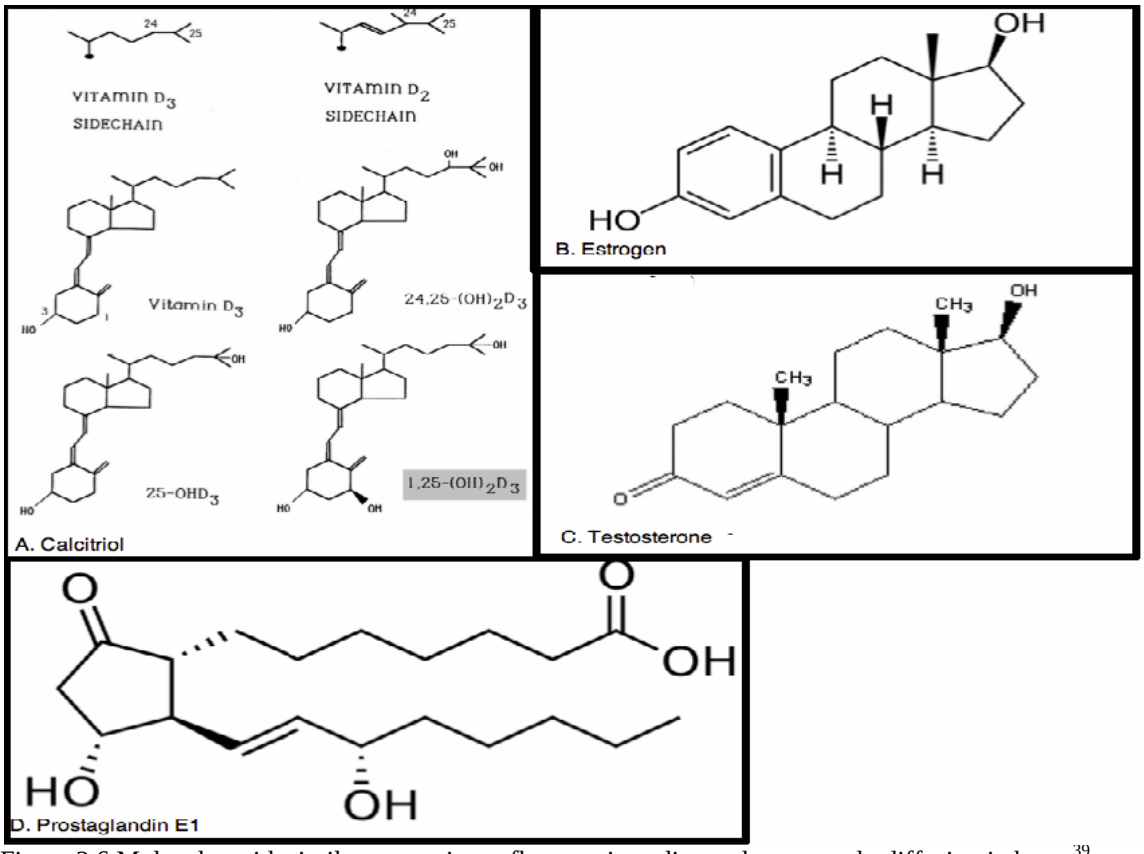

Figure 2.6 Molecules with similar properties to fluorescein sodium salt commonly diffusing in bone.[39]

The above figure illustrates various molecules with similar chemical properties to fluorescein. None of the molecules are structurally identical to fluorescein but all of them share amphipathic chemistries with fluorescein. All of the above molecules play an important role in homeostasis of bone tissue. Vitamin D is produced from cholesterol which shares chemistry with this group of bile salts and is plays an extremely important role in calcium absorption in bone. Important sex hormones, estrogen and testosterone, are also cholesterol derivatives that share similar chemistry with fluorescein. The environment that the fluorescein will be diffusing through has a large amount of lipids and some carbohydrates which will likely slow down diffusion due to its amphipathic properties just as is common in human bone tissue. In summary, fluorescein sodium salt

makes an ideal experimental molecule to quantify diffusion rates because of its similar biochemical interactions within bone tissue to the native factors that are commonly diffusing throughout human bone tissue.

2.8 Diffusion Coefficients in Water

As highlighted in Table 2.1, there are well established diffusion coefficients associated with fluorescein sodium salt and glucose in water. A study by *Periasamy et al.* worked with fluorescein sodium salt in water, focusing on relating photo-bleaching recovery data to transport phenomena[36]. The researchers mathematically modeled their data and used a fluorescent microscope to aid in defining the unknowns in their complex model and found that the diffusion of fluorescein sodium salt in phosphate buffer solution (PBS) was $2.7x10^{-6}$ cm^2/s[36]. The researchers felt that this number should be considered a benchmark, meaning any diffusion value within a biological tissue that creates a barrier to the rate of diffusion should always be lower than this calculated value of $2.7x10^{-6}$ cm^2/s[32]. Another highly respected study by Landolt-Bornstein in 1969 established the benchmark for the diffusion coefficient of glucose in water at $7.0x10^{-6}$ cm^2/s[37]. Our research will use these established benchmark numbers for comparative purposes.

CHAPTER III

METHODS

3.1 Acquisition and Preparation of Bone Samples

3.1.1 Animal Specifications

Canine bone samples were harvested from a sacrificed canine according to the specifications and guiding principles determined by the IACUC carried out by the Cleveland Clinic in 2007. Following sacrifice, the entire left tibia was dissected from the canine. The bone marrow was flushed out of the bone via phosphate buffer saline (PBS) irrigation. The tibia was then stored in a phosphate buffer saline with 0.05% sodium azide (Sigma) as an aseptic preservative at 4º C. The sample was labeled by year, type of animal, lot number of animal, and location of tissue in the canine; specifically, 07D-256 LEFT TIBIA.

3.1.2 Production of Bone Samples

After being removed from storage in the 4º C refrigerator, the bone was washed to remove all remaining layers of periosteum using a sterile towel and PBS solution to rub the surface of the bone. The end result was a bone sample consisting only of osseous tissue. Once clean, the bone was cut radially into six equal length sections (Figure 3.1). The two end sections were discarded because only the most medial sections were wanted for experimentation. The cutting was executed using a Labcut 1010 Low Speed Diamond Saw (EXTEC Corp). The saw's diamond blade was kept wet during cutting using a PBS solution to avoid dehydration and chipping of bone samples.

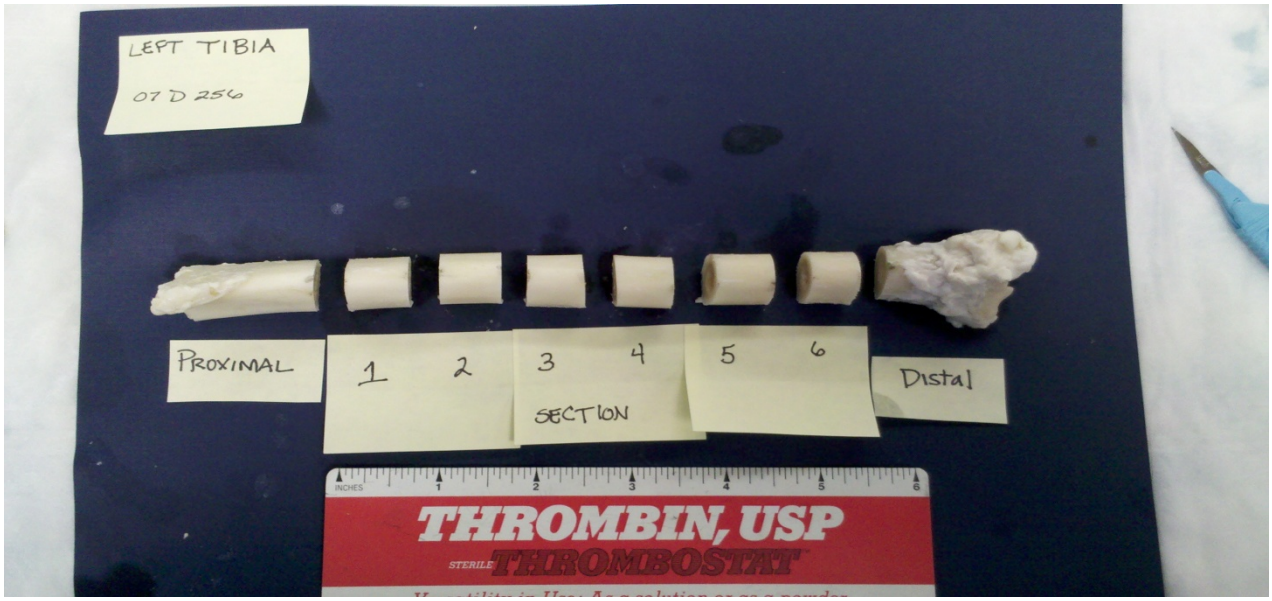

Figure 3.1 Canine tibia after initial cutting into sections.

Once the bone sample was cut into the six usable sections, each section was in turn used to cut three rectangular segments from the surface of the bone sample using a custom built jig designed specifically for the Labcut 1010 Low Speed Diamond Saw. The jig was a plastic guide-rail 3 cm tall and 10 cm long that ran parallel to the blade and allowed the user to make the desired cuts on each bone surface. The customizable part of

the jig was that the user could move it a distance of 1-10 mm from the blade depending on the size of the sample the operator needed. As the bone was being cut, the blade was again kept wet using a PBS solution.

First, the periosteal surface was axially cut off the surface on three sides of each of the six cylindrical bone sections to form a more triangular section of bone (Figure 3.2A). Then, the remaining endosteal surface was also axially cut from the three sides resulting in three rectangular segments of bone from each of the six sections (Figure 3.2B). In total, eighteen rectangular segments samples of bone, each approximately 1.7 cm x 1 cm x 0.3 cm, were created for experimental purposes (Figure 3.2C). Lastly, the endosteal face of each bone surface was marked with biocompatible paint to distinguish the positioning of the bone sample. The samples from each section were then placed into six separate Falcon tubes containing PBS with 0.05% sodium azide and were stored in a 4º C refrigerator until needed for the experiment.

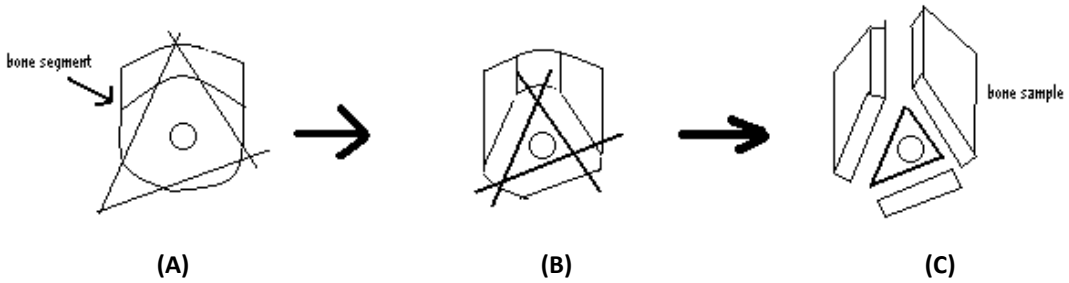

Figure 3.2 Schematic of bone sample production.

3.2 Sample Preparation

3.2.1 Encapsulation of Bone Sample

A hard, circular plastic tube (25 mm OD, 24 mm ID, 25 mm long) was used to prepare the bone sample. One end of the plastic tube was sealed with masking tape and a cuboidal bone sample was placed with the endosteal face on the tape as centrally in the tube as possible (Figure 3.3). Next, an orthodontic resin (Dentsply) was used to cover and seal all remaining exposed sides of the bone sample. The resin is a two-part epoxide consisting of a powder and a liquid used to make orthodontic retainers. The powder was spread on top of the bone to cover all exposed areas and fill the space between the bone sample and the tube walls. The liquid hardener was pipetted drop by drop until no powder remained, and the chemicals were gently mixed with a toothpick. This orthodontic resin is an epoxide that in previous experiments has been proven to be impervious to liquids and effectively bond to the surface of bone and not leach into porous materials, such as bone. Once the powder and liquid were mixed in the tube fully encapsulating the bone, it was allowed to harden for 24 hours.

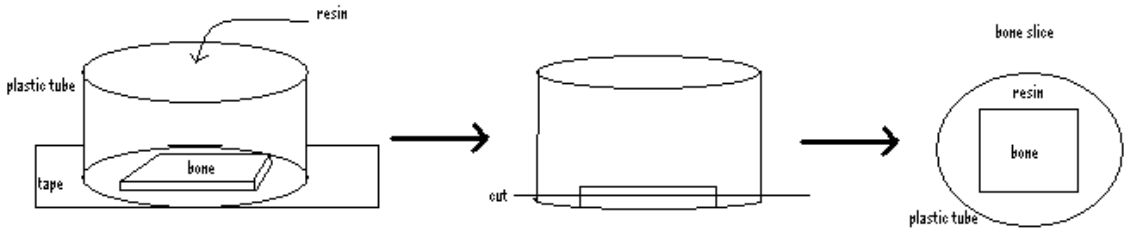

Figure 3.3 Schematic of bone encapsulation and bone slice cutting.

3.2.2 Bone Slice Cutting

Once the resin fully hardened for 24 hours, the masking tape was removed, exposing the endosteal surface of the bone sample. The surface was then rubbed with a

Kimwipe (Kimtech) soaked with PBS to moisten the bone and remove anything left behind by the masking tape. Using a low speed diamond saw (Buehler Isomet) kept wet using PBS, a slice was cut radially from the sample for use in the experiment (Figure 3.3). The approximate thickness of a slice was ~470 microns. After cutting the slice, the thickness was measured using a caliper at five different points around the slice and the average calculated. The newly cut slice was dabbed with a Kimwipe to remove excess PBS. Then, Krazy Glue (Elmer) was applied to the resin/bone and resin/plastic interfaces on the endosteal side of the sample using a disposable orthodontic brush (Henry-Schein) to seal the interfaces and ensure only diffusion occurs through the bone. Once sealed, the surface area available for diffusion was measured via a caliper at the edges of the glue-bone interface and some geometric calculations. The bone slice was then placed in a modified 25 mm filter holder (ADVANTEC) with the endosteal side facing the donor chamber. This filter holder was modified by fitting each end with a circular plastic piece designed to fit in the openings between the donor and receiver cells. Also, the tube fitting external to each side of the filter holder was removed to increase access to the sample.

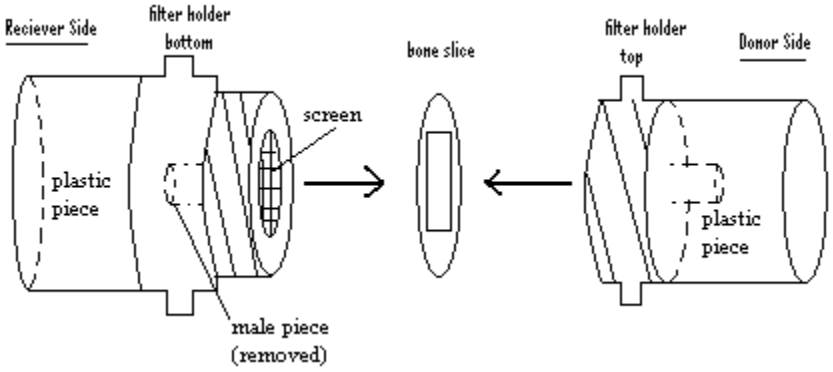

Figure 3.4 Schematic of placement of bone slice in the filter holder.

3.3 Preparation of Diffusion Solutions

The solutions used in the experiment were a PBS solution for the receiver chamber and a PBS/Fluorescein solution at varying concentrations for the donor chamber. The PBS solution was made in 2L batches by dissolving 16 g of NaCl (Fisher), 0.4 g of KCl (Sigma-Aldrich), 2.88 g of Na_2HPO_4 (Sigma-Aldrich), and 0.48 g of KH_2PO_4 (Sigma-Aldrich) in 1600 mL of deionized water. The pH was then adjusted to 7.4, and enough H_2O was added for a total volume of 2 L. The newly made PBS was then separated into two 1 L volumes: one to be kept as PBS, the other to make the PBS/fluorescein solution. To make the PBS/fluorescein solution, 0.1128 g of FITC (Sigma-Aldrich) was dissolved into the 1 L PBS to create a 300 µM solution. This solution was then be diluted with PBS depending on the desired molarity required for each trial. The two solutions were then autoclaved (Steris Amsco Lab 250) for 90 minutes to sterilize. The PBS/fluorescein bottle was wrapped in aluminum foil to prevent light damage to the fluorescent sodium salt and stored in the 4º C refrigerator until needed for experimentation.

3.4 Two Chamber Diffusion Tests

Diffusion trials were run in a custom two chamber diffusion cell (Crown Glass) connected to a 37º C water bath (Figure 3.5).

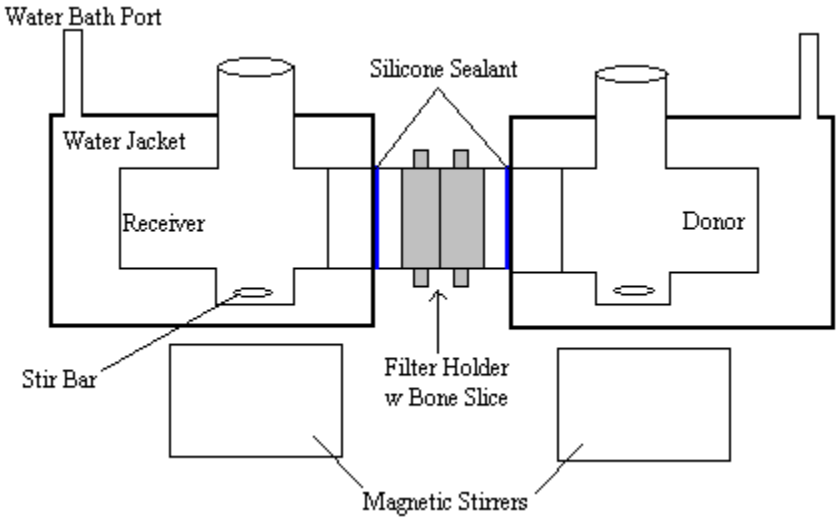

Figure 3.5 Schematic of diffusion cell system.

Once the sealed bone slice was placed into the filter holder with the endosteal surface of the bone facing the donor chamber, the diffusion cell was assembled and all possible points of leakage from the cells were sealed using 100% Silicone Aquarium Sealant (DAP Aquariums) and Stopcock Grease (Lubriseal)and held tightly together with a clamp. The diffusion cells were then placed on top of Micro-V magnetic stirrers (Cole-Parmer) to keep the cell solutions well mixed. Next, the receiver chamber was filled with 50 mL of the PBS solution and the donor chamber was filled with 50 mL of the PBS/Fluorescein solution at varying molarities depending on the trial. Molarities for the trials varied from 0.3-300 µM and the initial donor chamber concentration was changed from trial to trial to eliminate systemic error. Immediately, 1 mL was pipetted from each chamber and placed into 1.5 mL microcentrifuge tubes for baseline values, and labeled with the date and hour mark at which it was taken. The rest of the samples in the trial

were only taken from the receiver chamber. The time and date at which the trial began was recorded. The magnetic stirrers were then dropped into each cell and turned on for the entirety of the trial to ensure complete mixing. Finally, each diffusion cell was closed off at the top using a piece of Parafilm (BEMIS) so no evaporation out of the cell could occur. The lights were kept off in the laboratory as much as possible to prevent light damage to the fluorescent sodium salt in the solutions.

Samples were taken from the receiver cell approximately every 24 hours for 7-10 days using a transfer pipette (Fischer Brand) and placed into a 1.5 mL sample tube. These tubes were then stored in a dark 4º C refrigerator to prevent light damage until needed for measurement in the F-7000 Fluorescence Spectrophotometer (Hitachi).

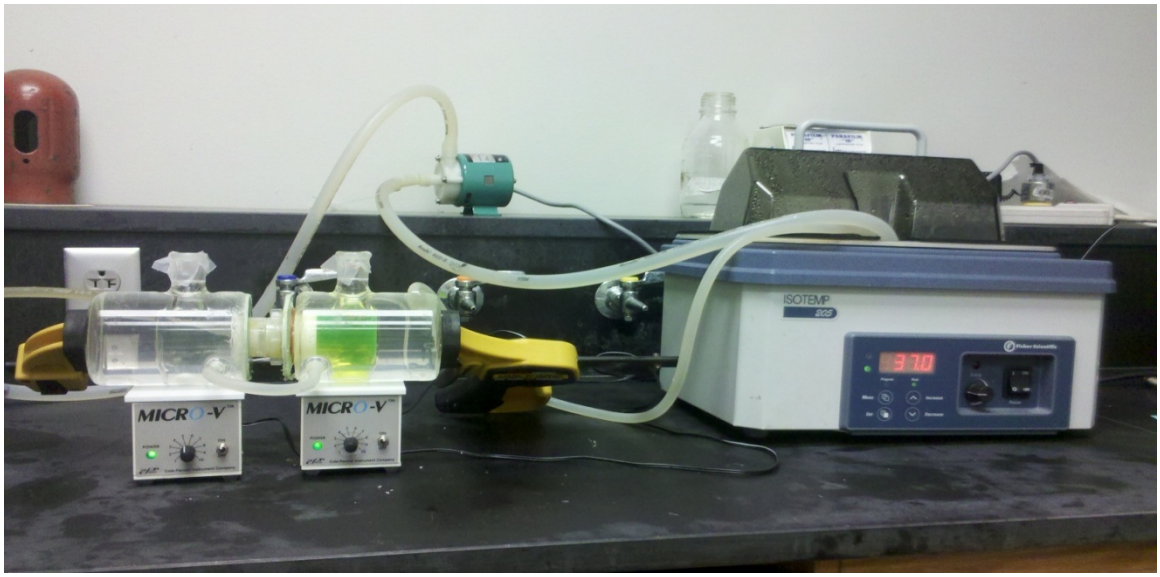

Figure 3.6 Diffusion Cell System.

3.5 Preparation for Analysis

3.5.1 Calibration Curve Sample Preparation

A calibration curve was made on the fluorometer for analysis of the fluorescein concentration in the PBS solution. The samples for making the calibration curve were created using a solution of 0.3 µM fluorescein in PBS, and diluted successively 1:1 nine times for a total of ten samples for the curve. Specifically, 2 mL of 0.3 µM fluorescein solution was placed in a cuvette. Next, 1 mL was pipetted out and placed in a second cuvette containing 1 mL deionized H_2O and mixed. From that cuvette, 1 mL was pipetted out and placed in a third cuvette containing 1 mL deionized H_2O and mixed. This continued for a total of ten cuvettes to make the calibration curve.

3.5.2 Sample Dilution

Depending on the fluorescein concentration solution used, there were two different methods of preparing the samples for measurement in the fluorometer. Trials using a concentration of 0.3 µM were immediately ready for analysis due to their low concentration. However, trials ran using a concentration of 30 µM or 300 µM needed to be diluted to fit within the range of the calibration curve. For samples needing dilution, 1 mL sample was pipetted into a 15 mL centrifuge tube (Corning) and 9 mL of deionized H_2O was added and shaken for a 1:10 dilution. Samples from trials at 30uM were diluted once, 1:10, while samples at 300uM needed a 1:20 dilution. Once the samples were diluted, they were ready to be analyzed by the fluorometer.

3.6 Data Acquisition Using Fluorescence Spectrophotometer

All fluorescence data were acquired using a Hitachi F-7000 Fluorescence Spectrophotometer in the Chemistry Lab at Cleveland State University. Protocol for use of the fluorometer was specified and written by Dr. Zhou of the Department of Chemistry at Cleveland State University. To begin, the PC and fluorometer were powered on and the xenon lamp was allowed to warm up for 30 minutes. Once the lamp was ready and warm, the FL Solutions Program was opened and allowed to initialize. Once the status bar turned green, the program was ready for use. Under the Method section, measurement mode was set to Photometry, quantitation type set to 1^{st} Order Wavelength, and instrument mode set at Fluorescence with fixed Excitation/Emission Wavelengths at 494 nm and 518 nm respectively. The Standards tab was then selected and the ten concentrations for the calibration curve were entered. Next, under the Samples tab, the number of samples to be measured and the name of the sample were entered. In this case, the names were the hour at which the sample was taken during the specific trial. After all this setup was performed, the samples were ready for measurement by clicking the Measurement button. First, the program asked for the calibration standards to be measured to produce the calibration curve. The first standard, 0.3 µM, was placed in the cuvette port and the lid closed. On the computer screen it read, “Press OK when ready to measure” so “OK” was pressed and the program measured the fluorescence in units of intensity and displayed it on the screen and also began to create a calibration curve. The program then instructed to remove the standard and place the next standard in the cuvette port for measurement. Once all of the standards were measured and the calibration curve completed, the program asked to move on to the sample measurement. Beginning with

the “0hr receiver chamber” sample, 1 mL from each sample was placed into a cuvette and measured by the fluorometer in the same fashion as the standard measurements. Once everything was measured, the program gave the user three sheets to print out: a graph of the calibration curve with units of concentration on the x-axis and intensity on the y-axis, a readout of the standards name and intensity measurements, and a readout of the samples names and intensity readouts. These readouts were then entered into Excel to convert intensity to concentration in order to produce a concentration curve and overall diffusion coefficient for each trial.

3.7 Transport Model

The transport model for this experimental set-up was derived based on the section *Quasi-Steady State Transport* in chapter 6.8 of *Truskey et al*[15]. The bone tissue used in the experiment had an area *A* and a thickness *L* that separated two solutions of volumes V_1 and V_2. At times less than zero, all concentrations in the chambers and tissue equal zero. The fluorescein concentration in PBS in the donor chamber is represented by C_D, and the fluorescein concentration in PBS in the receiver chamber, C_R, are both functions of time, t. At time equal to zero, the fluorescein concentration in the donor cell was raised to a concentration of C_o, while the concentration of the receiver chamber, C_R, remained zero, yielding the initial conditions:

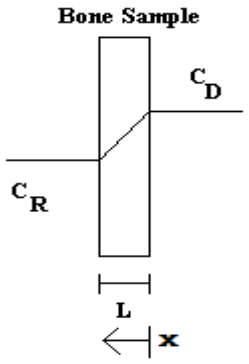

@ t = 0 $\quad C_D = C_o$

$C_R = 0$ [1]

Based on the boundary and initial conditions in the bone sample,

$x \geq 0$	$t \leq 0$	$C_{Bone} = 0$	[2.1]
$x = 0$	$t \geq 0$	$C_{Bone} = C_D\Phi$	[2.2]
$x = L$	$t \geq 0$	$C_{Bone} = C_R(t)\Phi$	[2.3]

In order to apply quasi-steady state analysis, the timescale by which the surface concentration changes (t_c) must be much slower than the timescale for diffusion across the bone sample ($t_{D,bone}$). In other words, it was assumed that the diffusion in the bone is much faster than the transport rate that leads to the solute concentration at the boundaries to change:

$$t_{D,bone} << t_c$$

It can be shown that the characteristic diffusion time is proportional to $L^2/D_{Fluorescein}$. The relationship of $t_{D,bone} << t_c$ was assumed to be satisfied based on the fact that the volume of the bone tissue is much less than the volume of the diffusion cell chambers. With this assumption, steady-state transport across the bone tissue can be assumed.

A steady-state mass balance of solute within the bone sample yields:

$$0 = D_{Bone}\frac{d^2C_{Bone}}{dx^2} \qquad [3]$$

Next, equation 3 was integrated and combined with the flux ($J_{Fluorescein}$) from Fick's Law to obtain the overall equation:

$$J_{Fluorescein} = -D_{Bone}\frac{dC_{Bone}}{dx} = \frac{D_{Bone}\Phi}{L}(C_D - C_R) \qquad [4]$$

The partition coefficient, Φ, was assumed to equal 1 (See Section 4.4). Next, a mass balance was applied to the donor chamber and the later part of equation 4 was substituted in for $J_{Fluorescein}$ to acquire:

$$-V_D \frac{dC_D}{dt} = \frac{A_{Bone} D_{Bone} \Phi}{L}(C_D - C_R) \qquad [5]$$

The concentrations C_D and C_R were related by observing that after the solute left the donor chamber, it was either in the bone tissue or in the receiver chamber. By conservation of mass, the loss of the solute in the donor chamber is balanced out by the gain of solute in the bone tissue or the receiver chamber; mathematically:

$$V_1 \frac{dC_D}{dt} = -\left(\frac{V_{bone}}{\Phi} \frac{dC_{bone}}{dt} + V_2 \frac{dC_R}{dt} \right) \qquad [6]$$

Given that $V_1 = V_2 = V$, and $V_{Bone} << V$, then the first term on the right hand side is much less than the other two terms. Therefore, the amount of solute in the bone tissue is very small relative to the amount of solute in either chamber and as a result the above equation can be simplified to:

$$\frac{dC_D}{dt} = -\frac{dC_R}{dt} \qquad [7]$$

Using the initial conditions from equation 1, the above equation was integrated to yield:

$$C_D - C_o = -C_R \qquad [8.1]$$

or

$$C_D = C_o - C_R \qquad [8.2]$$

Next, equations 7 & 8.2 were substituted into equation 5 to acquire a differential equation in one variable:

$$V \frac{dC_R}{dt} = A_{Bone} D_{Bone} \Phi \frac{(C_o - 2C_R)}{L} \qquad [9]$$

Integrating equation 9 and applying the initial condition (equation 1) resulted in the overall diffusion equation for the experiment:

$$\ln\left(\frac{C_o - 2C_R}{C_o}\right) = -\frac{2A_{Bone}D_{Bone}\Phi t}{VL} = BD_{Bone}t \qquad [10]$$

The steady-state concentrations equal $C_o/2$ in each chamber. A graph of $\ln[(C_o-2C_R)/C_o]$ vs. t is thus expected to be linear with a slope equal to $-2A_{Bone}D_{Bone}\Phi/VL$ which provided a straightforward method of determining the diffusion coefficient. The slope and the standard error of the slope were calculated via the LINEST function in Microsoft Excel and each were divided by the physical parameters, or the B parameter, which is equal to $-2A_{bone}\Phi/VL$ in order to find the diffusion coefficient.

CHAPTER IV

RESULTS AND DISCUSSION

The following sections will present the data obtained for each trial performed in the experiment. Before the data is presented, it is necessary to describe the terminology used in the ensuing chapter. The full canine tibia was cut in to 8 sections as seen in Figure 3.1, and marked as "Section #". Once the bone was cut into the 8 sections, the two end pieces were discarded and the interior 6 sections were available for use in the experiments. Once a bone section was chosen for use, the periosteal layer was removed and a slice was cut from the endosteal tissue for use in the diffusion chamber. Each slice is labeled "sample #" and each subsequent experimental run is labeled "trial #". When put all together, each trial performed is labeled by section/sample/trial. For example, the first experimental data is labeled "4.1.1" because the bone tissue comes from the 4th section, it is the

first sample taken from the 4th section, and it is the first trial run on that specific bone slice.

4.1. Sample Results

Two control trials were run prior to running all of the actual diffusion trials. These control trials were run to test for leaks in the diffusion cell system and to determine if the orthodontic resin and Krazy Glue were impermeable to diffusion. The first trial run was strictly for visual confirmation. A typical bone slice such as used in the actual trials was used, but the entire endosteal surface of the bone was covered with Krazy Glue, as well as the bone-resin and resin-plastic interfaces. Instead of fluorescein in the donor chamber, a bright red food dye was used for visual purposes to determine if any diffusion were occurring over the seven day period. After seven days, the PBS in the receiver chamber was still as clear as it was to begin with.

The second control trial was similar to the first trial run; with the exception of a 300 μM PBS/fluorescein solution was put in the donor chamber in place of the red food dye. Measurements were taken every 24 hours for seven days to test for diffusion. Figure 4.1 shows the concentration curve generated by the second control trial. The graph shows basically a flat line indicating that no diffusion through the bone sample into the receiver chamber occurred over the seven days.

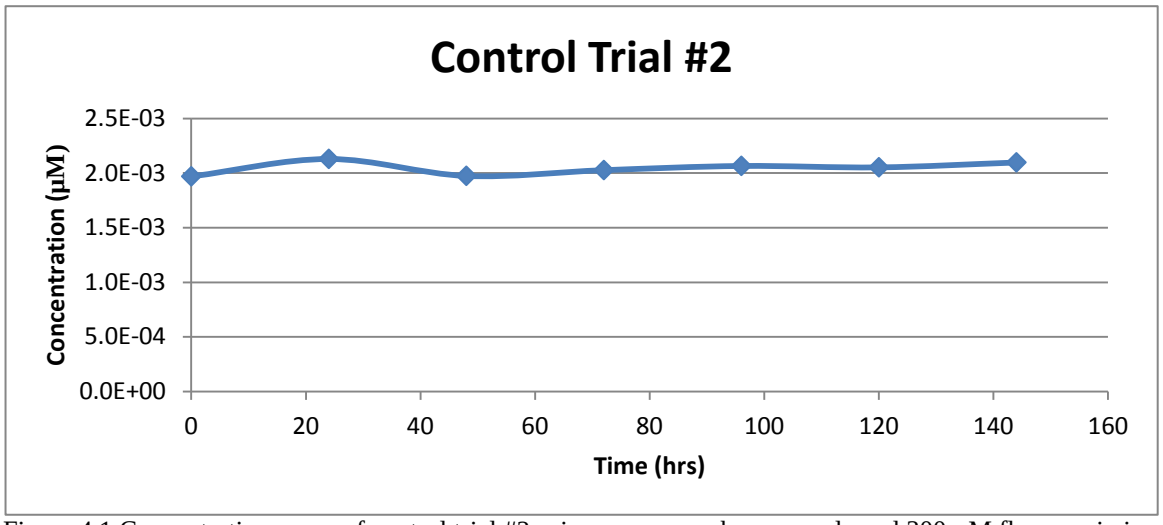

Figure 4.1 Concentration curve of control trial #2 using nonporous bone sample and 300 µM fluorescein in PBS.

Figure 4.2 illustrates a sample calibration curve produced by the fluorescence spectrophotometer using the ten standard concentrations described in Section 1.5.1. A calibration curve using these ten standards was generated each time the fluorometer was used to measure FITC concentration in the samples from the receiver chamber.

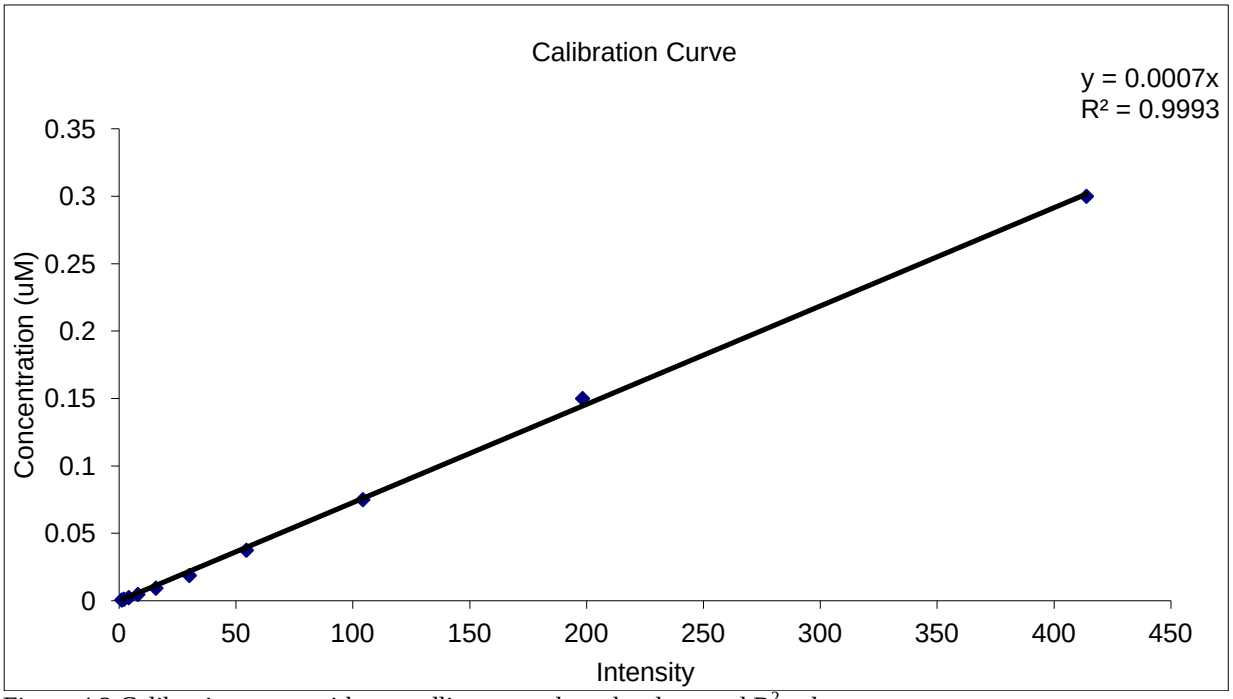

Figure 4.2 Calibration curve with a trendline to produce the slope and R^2 value.

A sample result is shown in Figure 4.3, which shows the fluorescein concentration in the receiver chamber from trial 13 on bone tissue sample #1 from bone section 4.

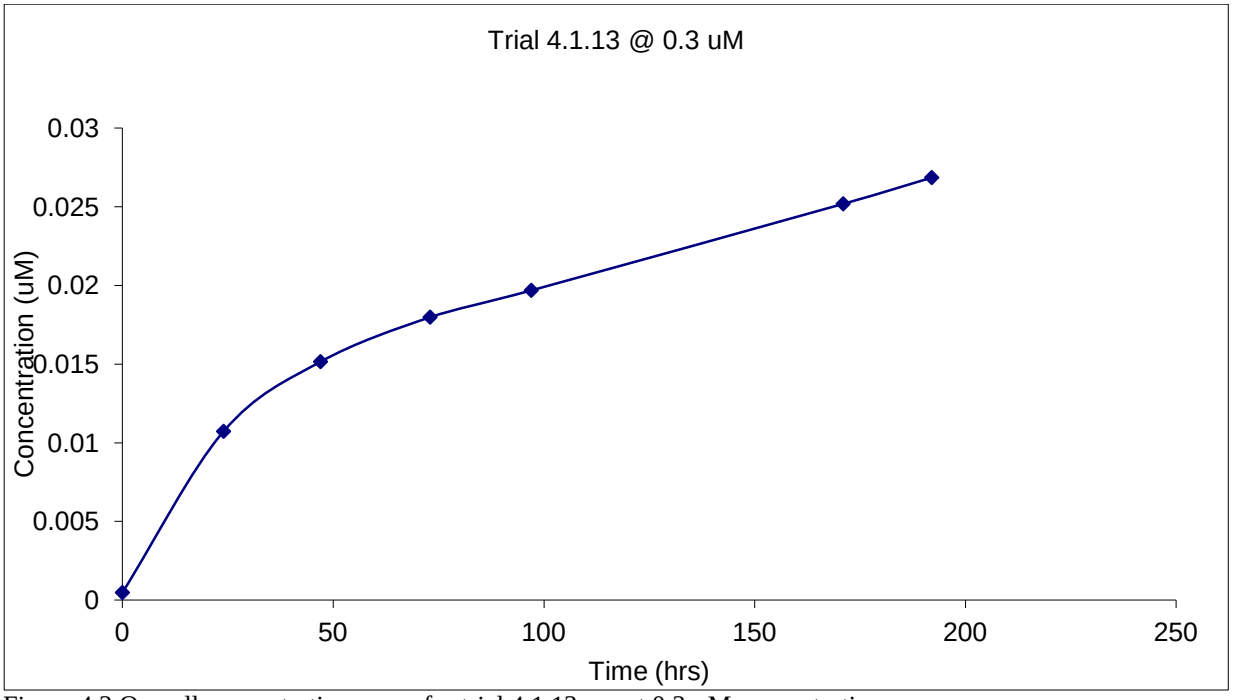

Figure 4.3 Overall concentration curve for trial 4.1.13 run at 0.3 µM concentration.

The fluorescein concentration in the receiver chamber was used to create a graph of $\ln((C_o-2C_R)/C_o)$ vs. time, according to the model equation 10 (Figure 4.4). The LINEST function in Microsoft Excel was used to produce the slope and error (see section 1.8). Both the slope and the error generated via the LINEST function were divided by the B parameter ($B=-2A_{Bone}/[VL]$) to calculate the diffusion coefficient and error for the trial, according to equation 10.

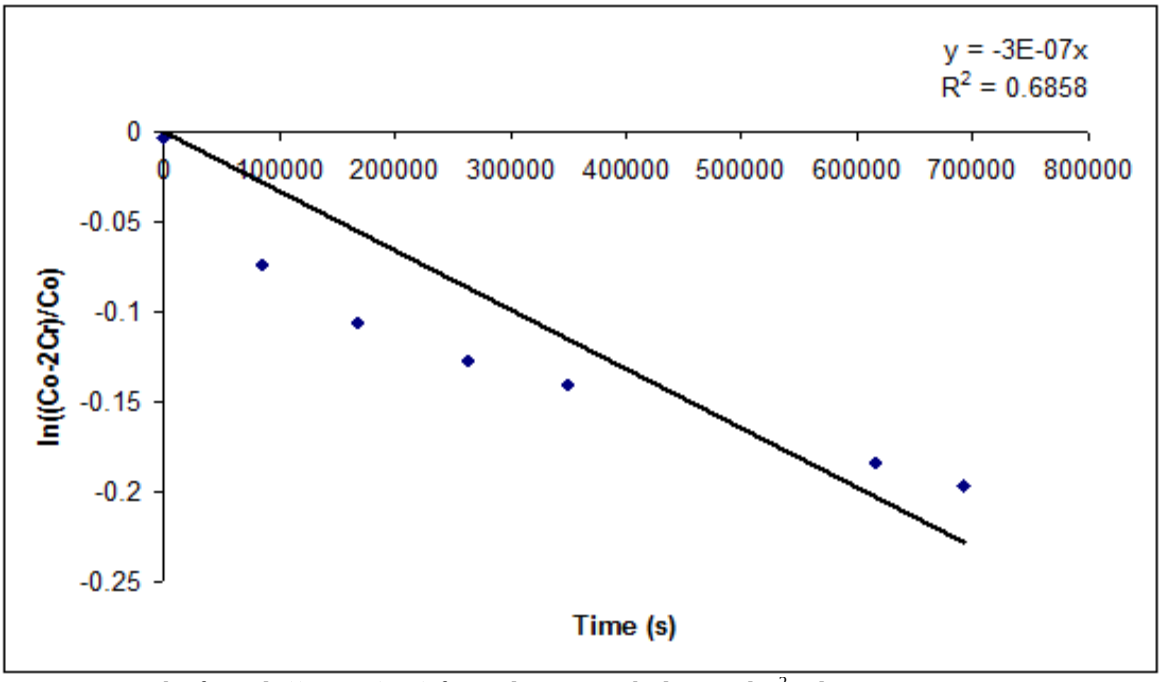

Figure 4.4 Graph of t vs. $\ln((C_o-2C_R)/C_o)$ for trial 4.1.13 with slope and R^2 value.

The slope of this example data in Figure 4.4 is $-3.29\text{x}10^{-7}$ s^{-1} with an error of $\pm 3.58\text{x}10^{-8}$ s^{-1}. From the system geometry, thickness and area of the bone sample, and initial donor concentration for trial 4.1.13, the B parameter was calculated to be -1.494 cm^{-2}. The ratio of the slope to the B Parameter produces the diffusion coefficient and its error: $2.20\text{x}10^{-7} \pm 2.39\text{x}10^{-8}$ cm^2/s.

a.)

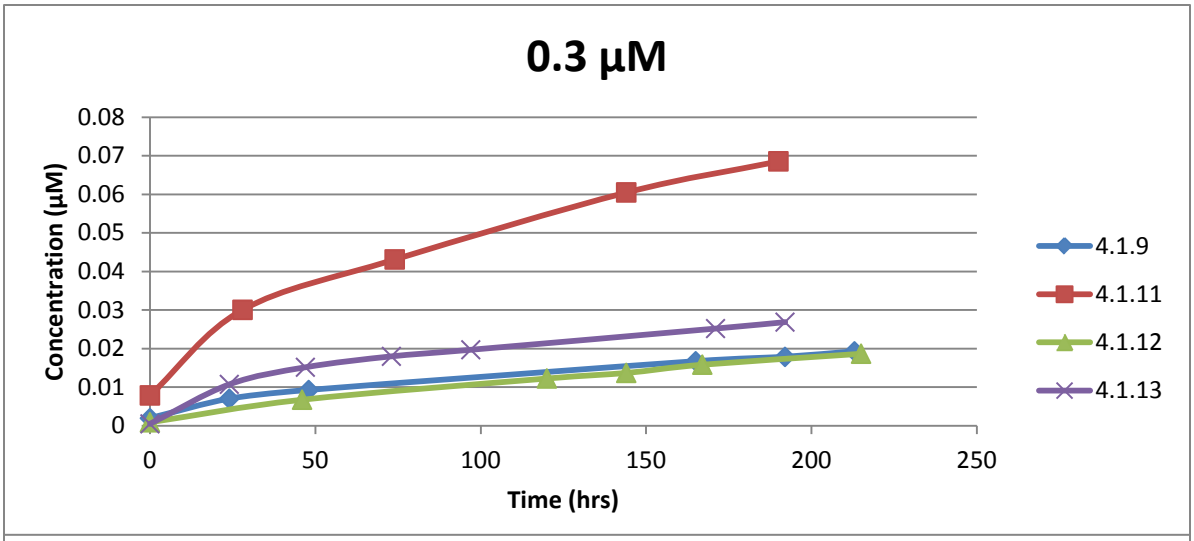

b.)

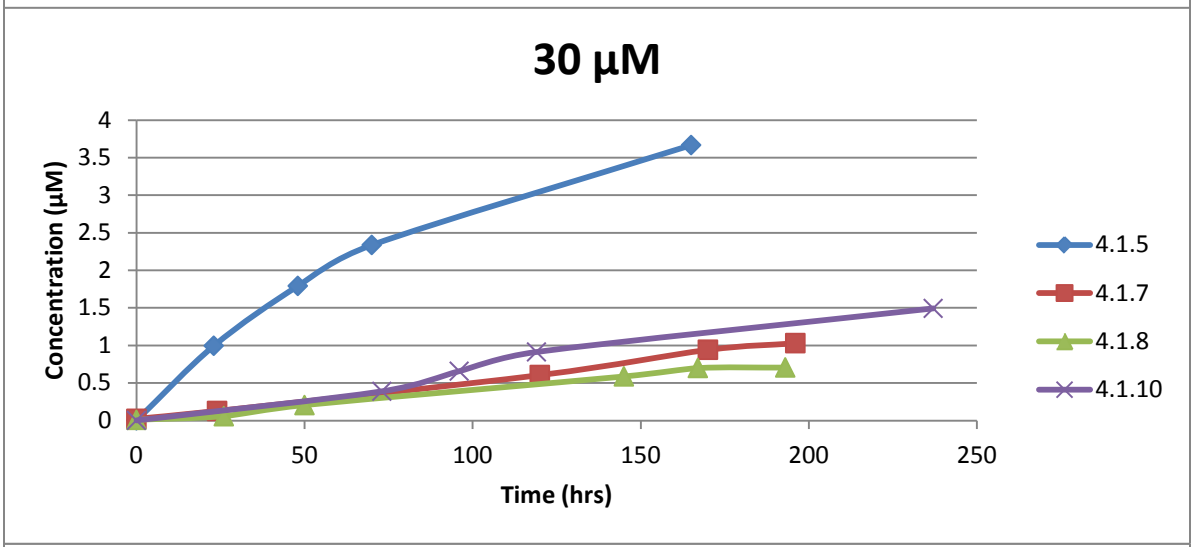

c.)

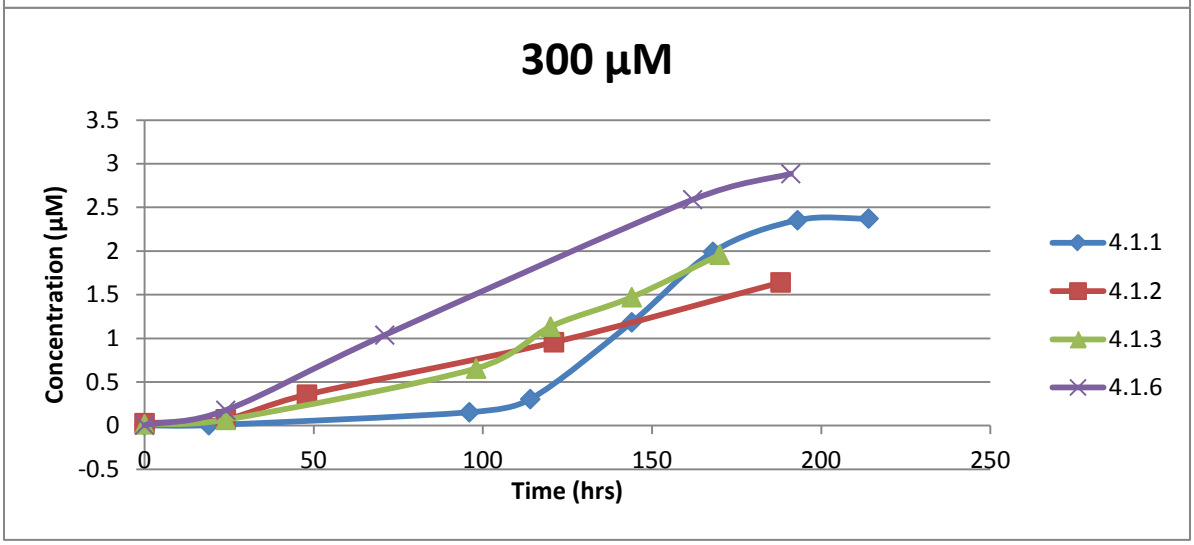

Figure 4.5 a.) Concentration curves for trials run at 0.3 µM. b.) Concentration curves for trials run at 30 µM. c.) Concentration curves for trials run at 300 µM.

Figure 4.5 displays all of the concentration curves generated for each trial at each initial donor concentration. Figure 4.5a shows concentration curves for trials run with an initial donor concentration of 0.3 µM. These curves all have all have the same trend. Each curve has a large increase up to around 50 hours, then slightly levels out for a steady increase to the end of the trial. Trials 4.1.9 and 4.1.12 both have very similar numbers throughout. Trial 4.1.13 has the same trend as those two but has a larger increase in concentration in the first 50 hours. Trial 4.1.11 has the same trend as the other three, however it has a much larger increase in concentration and was considered an outlier (discussed later).

Figure 4.5b shows the concentration curves for trials run with an initial donor concentration of 30 µM. Excluding trial 4.1.5 which was considered an outlier, the other three trials all had a relatively steady and consistent increase in concentration throughout their trials. Trial 4.1.8 started slow but between 24-50 hours saw a large increase in concentration that continued steadily until it leveled off around 170 hours. Trial 4.1.7 had a very steady and linear concentration profile throughout. Trial 4.1.10 started the same as trial 4.1.7 but around 75 hours saw a large spike in concentration compared to the other two trials.

Figure 4.5c shows the concentration curves for trials run with an initial donor concentration of 300 µM. These trials saw the most variation in the concentration curves compared to the other experimental concentrations. Trial 4.1.1 saw a very slow start until around 100 hours, then had a huge spike in concentration for the rest of the trial. Trial 4.1.2 started increasing around 24 hours then maintained a steady linear increase throughout. Trial 4.1.3 also saw an increase around 24 hours, but also saw a jump at

around 100 hours that continued throughout. Trial 4.1.6, like 4.1.2 and 4.1.3, didn't increase until around 24 hours. However, its initial increase was larger and maintained its larger values throughout its duration.

Over the eight day period of each trial, the receiver chamber only ever reached a maximum of around one tenth the concentration of the donor chamber. If the trials were allowed to run for a longer period of time, the concentration of the receiver chamber would continue to increase until equilibrium were reached.

4.2 Diffusivities as a Function of Solute Concentration

a.

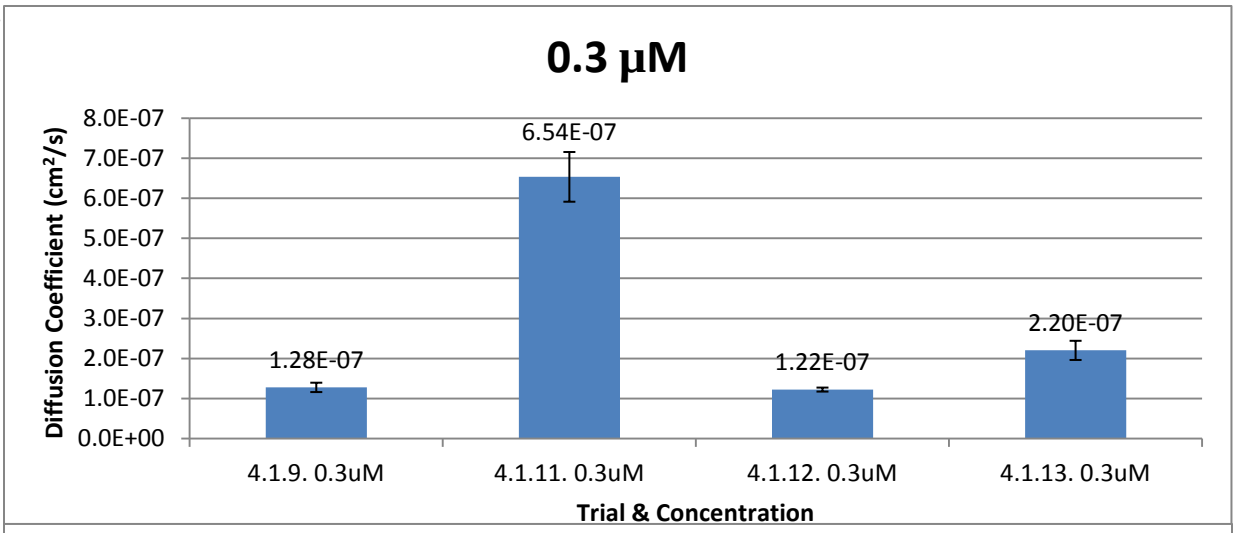

b.

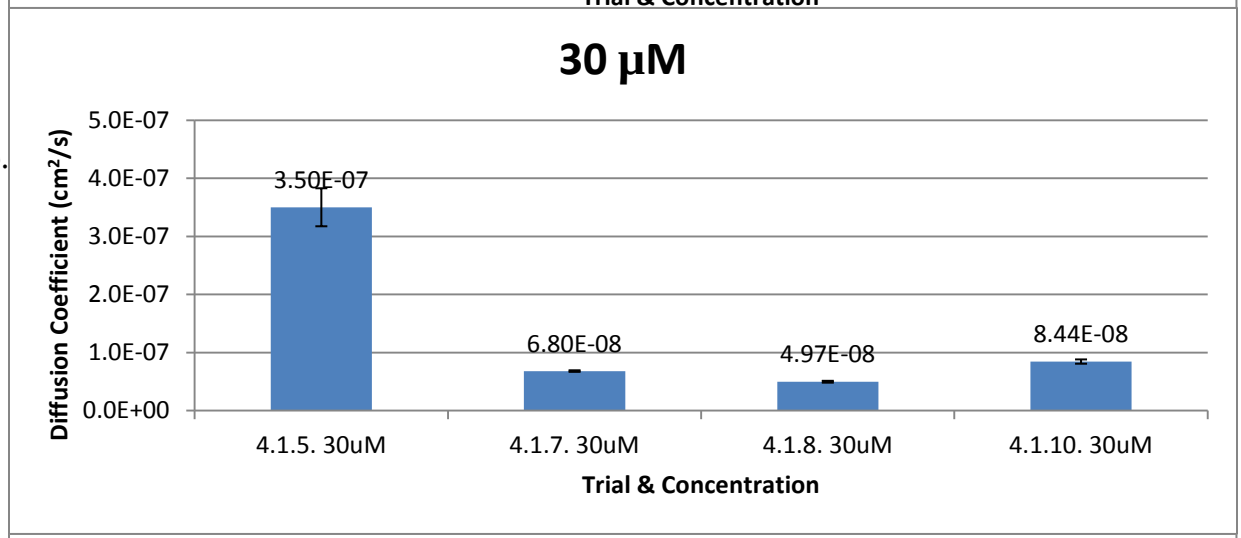

c.

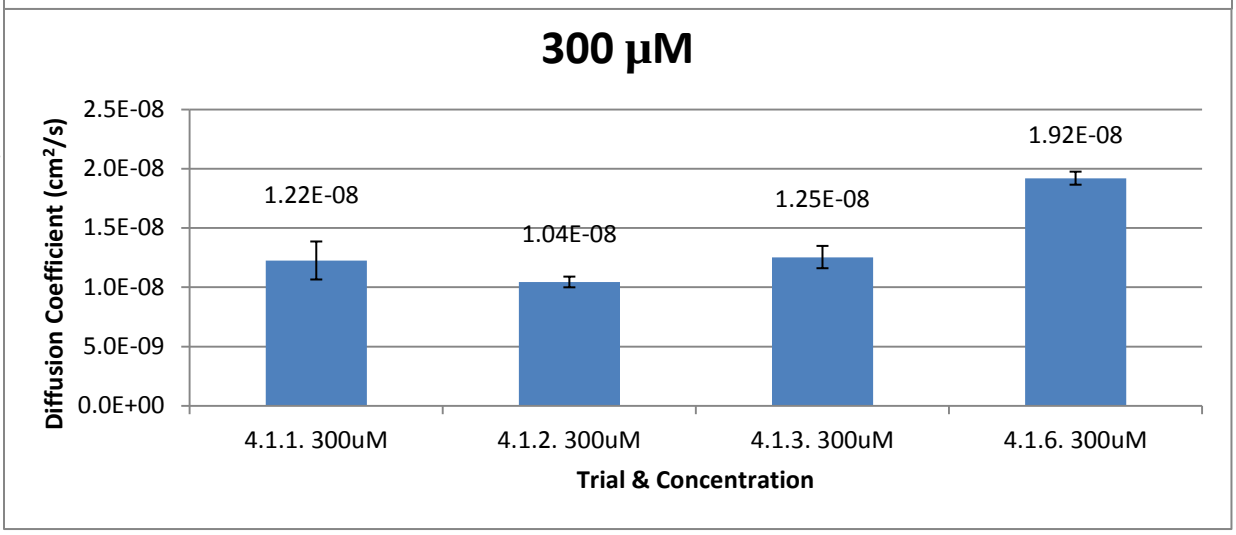

Figure 4.6 a.) Diffusion coefficients for trials run at 0.3 µM. b.)Diffusion coefficients for trials run at 30 µM. c.)Diffusion coefficients for trials run at 300 µM. The error bars represent the standard error of the slope of the $\ln((C_o-2C_R)/C_o)$ vs. time graphs for each trial.

The diffusivities for one sample from section 4 of the canine tibia are shown at three different initial fluorescein in PBS concentrations (0.3, 30, and 300 µM) in Figure 4.6 (a-c).

Figure 4.6a displays the diffusion coefficients for trials run with an initial donor chamber concentration of 0.3 µM. The average value of the diffusion coefficient of 0.3 µM fluorescein in PBS through bone was found to be 2.81×10^{-7} $cm^2/s \pm 1.28 \times 10^{-8}$ cm^2/s. However, 4.1.11 was considered an outlier due to it being fivefold higher than the other trials at this concentration. With trial 4.1.11 disregarded, the average diffusion coefficient for 0.3 µM trials was found to be 1.57×10^{-7} $cm^2/s \pm 3.17 \times 10^{-8}$ cm^2/s. Disregarding trial 4.1.11, the trials run at 0.3 µM in section 4 ranged from 1.22×10^{-7} to 2.20×10^{-7} cm^2/s. These trials had an average error of around 8.02%.

The average value of the four measurements of the diffusion coefficient of 30 µM fluorescein in PBS through bone section 4 was found to be $1.38 \times 10^{-7} \pm 7.65 \times 10^{-9}$ cm^2/s. The second graph, Figure 4.6b, displays the diffusion coefficients for all trials run at 30 µM in bone section 4. However, if trial 4.1.5 were removed and considered an outlier due to it being over fivefold higher than the other trials performed at this concentration, the value of the diffusion coefficient was found to be $6.74 \times 10^{-8} \pm 1.00 \times 10^{-8}$ cm^2/s. Another reason why trial 4.1.5 was removed was because an older PBS/Fluorescein solution (> 1 year old) made for a previous student's research was used while new solutions were being made. After discarding the outlier trial 4.1.5, the diffusion coefficient values for trials run at 30µM in bone section 4 ranged from 4.97×10^{-8} to 8.44×10^{-8} cm^2/s. These trials had an average error of around 3.17%.

Figure 4.6c displays the diffusion coefficients for trials run with an initial donor chamber concentration of 300 µM. The average value of the diffusion coefficient for trials run at 300 µM fluorescein in PBS through bone was found to be $1.36x10^{-8}$ ± $1.93x10^{-9}$ cm^2/s. Calculated diffusion coefficients for trials run at 300 µM ranged from $1.04x10^{-8}$ to $1.92x10^{-8}$ cm^2/s. The diffusion coefficients at 300 µM were the most consistent of the three experimental concentrations and had an average error around 6.96% among the trials.

The results of the diffusion trials were statistically analyzed by comparing concentration groups via a 2-tailed t-test, unpaired data, equal variances, using an $\alpha=0.05$ (95% confidence limit). The t-test compared trials at 0.3 µM vs. 30 µM vs. 300 µM. The analysis between 0.3 µM and 30 µM showed a statistical difference and there was also a statistical difference between 30 µM vs. 300 µM (Figure 4.7). The results of the t-test confirmed that the three concentration groups (0.3, 30, and 300 µM) and their trials are statistically different from one another and the three sample populations can neither be grouped nor averaged together.

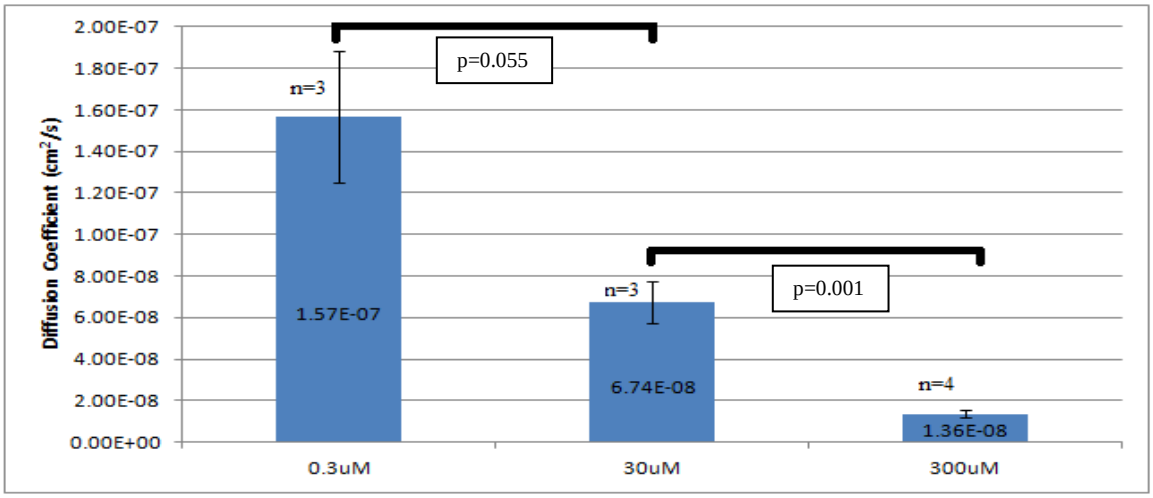

Figure 4.7 Comparison of diffusion coefficients for trials run at 0.3 µM vs. 30 µM vs. 300 µM. The error bars represent the standard error of the measurements for each trial. P-values in the figure represent t-test using equal variance. Using unequal variance, p=0.115 for 0.3 µM vs. 30 µM and p=0.034 for 30 µM vs. 300 µM.

4.3 Effect of Location on Diffusion Coefficient

a.

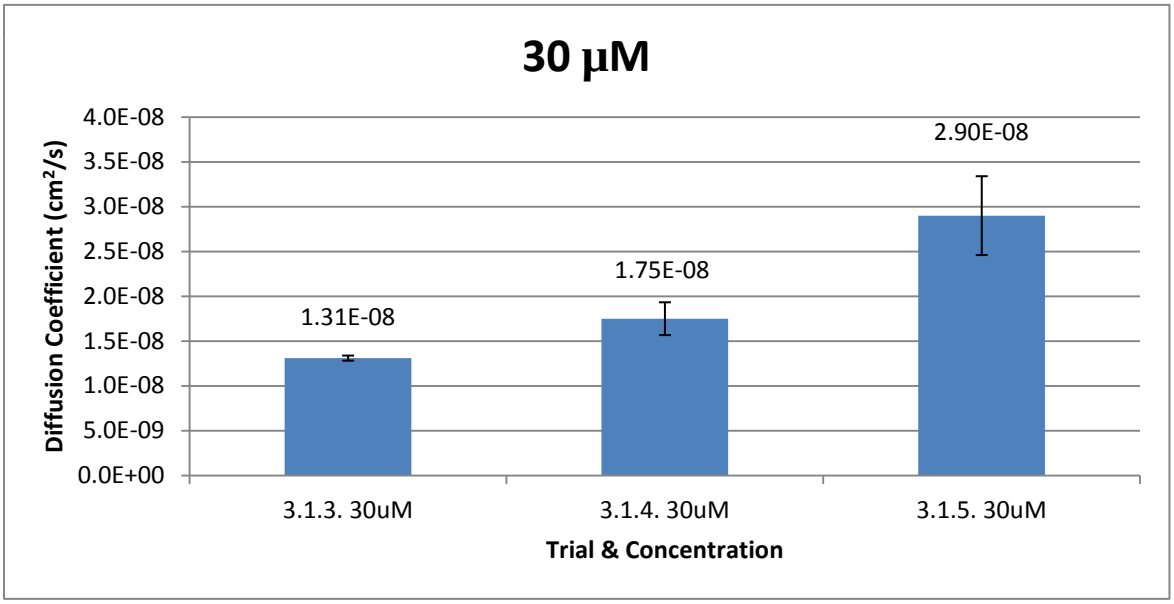

b.

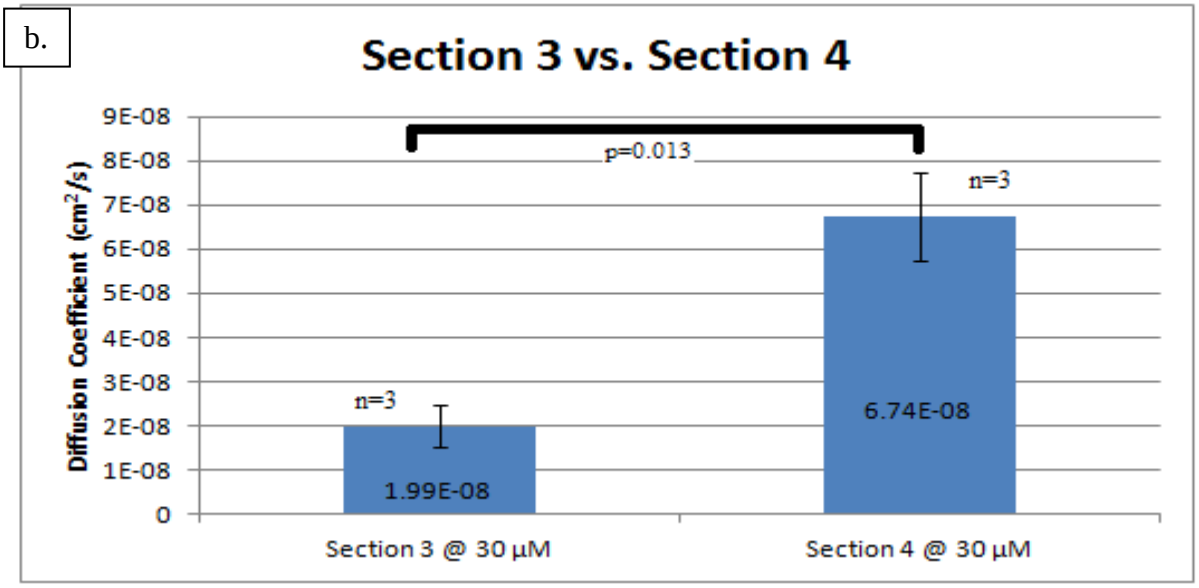

Figure 4.8 a.) Diffusion coefficients for trials run at 30 µM in bone section 3. b.) Comparison of the diffusion coefficients run at 30 µM in bone section 4 vs. bone section 3.P-value using equal variance was P=0.013. P-value for comparison was 0.023 at unequal variance. The error bars represent the standard error of the measurements for each trial.

Once there were sufficient trials performed on the sample from bone section 4, it was removed from the diffusion apparatus and replaced with a sample from bone section 3. The idea was to run trials on a bone sample from a different part of the canine tibia and attempt to reproduce the numbers from the previous trials on bone section 4. Trials 3.1.3-

3.1.5 were run with an initial donor chamber concentration of 30 µM. Figure 4.8a shows the values for the diffusion coefficients measured for each trial run on bone section 3. The average value of the diffusion coefficient of 30 µM FITC in PBS through bone section 3 was found to be $1.99x10^{-8} \pm 4.74x10^{-9}$ cm^2/s. The diffusion coefficients for trials run at 30 µM in bone section 3 ranged from $1.31x10^{-8}$ to $2.90x10^{-8}$ cm^2/s. These trials had an average error of around 9.26%.

The results of the diffusion trials were statistically analyzed using a 2-tailed t-test, unpaired data, equal variances, using an $\alpha=0.05$ (95% confidence limit) comparing bone section 4 and bone section 3 (figure 4.8b). The results of the t-test showed a statistical difference ($P=0.013$) between bone section 4 and bone section 3. The experimental test results show that the position on the bone, proximal/distal, have an effect on the diffusion coefficient. Sections 3 and 4 were both taken from the most medial part of the tibia, with Section 3 being more proximal and Section 4 more distal (Figure 3.1). The more proximal Section 3 gave a lower overall diffusion coefficient than the more distal Section 4 allowing for it to be determined that, in this thesis experiment, diffusion is less limited in the more distal portions of the canine tibia.

Bone section 3 trials were also run in conjunction with *Gonzalez's*[40] research to see if similar diffusion coefficients could be obtained by two different techniques. Both techniques used a bone sample from the same bone section (section 3) and the same initial FITC in PBS concentration (30 µM) to find a diffusion coefficient. *Gonzales'* technique, which is the same technique as *Farrell*[39], used fluorescence imaging and MATLAB to obtain diffusion coefficients for fluorescein in PBS at 30µM in the bone sample[40]. The average overall diffusion coefficient measured in this experiment for the

bone section 3 trials was $1.99x10^{-8} \pm 4.74x10^{-9}$ cm^2/s. The average overall diffusion coefficient measured in *Gonzalez's* experiment for bone section 3 trials was $3.28x10^{-8} \pm 6.58x10^{-9}$ cm^2/s. Although two different methods of measuring the diffusion coefficient were used, very similar numbers were calculated. The results of the diffusion trials were statistically analyzed using a 2-tailed t-test, unpaired data, equal variances, using an α=0.05 (95% confidence limit) comparing the results from the two different techniques. The results from the t-test confirmed that the two groups of number are statistically similar (P=0.179) to one another and the two sample populations can be grouped and averaged together giving an average overall diffusion coefficient of $2.92x10^{-8}$ $cm^2/s \pm 5.38x10^{-9}$ cm^2/s.

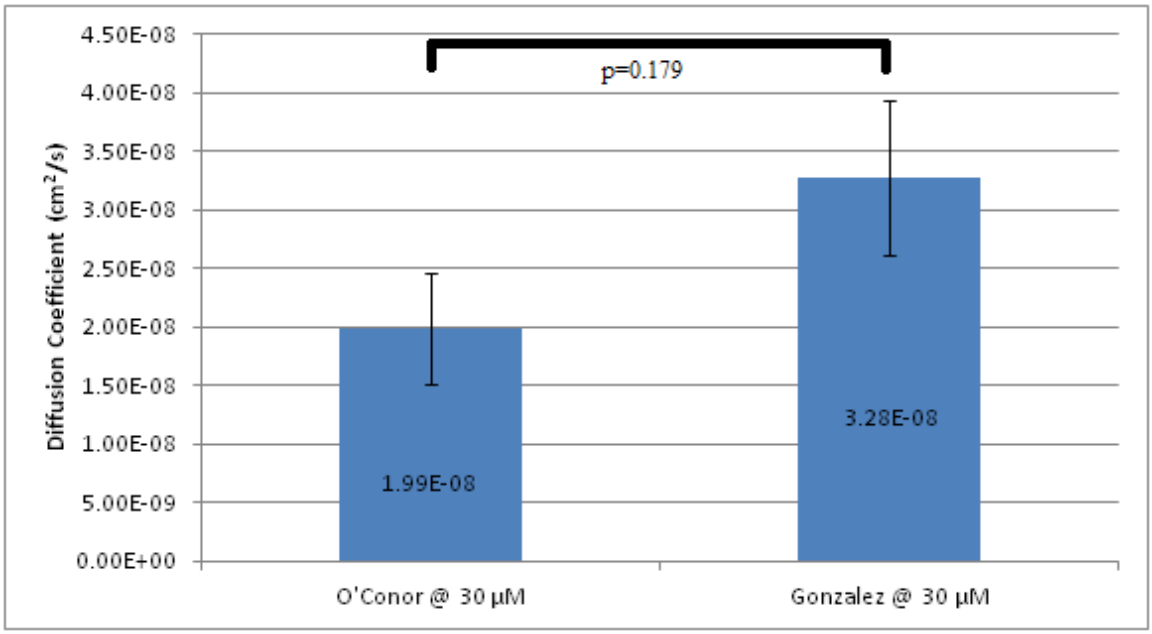

Figure 4.9 Bone section 3 diffusion coefficients measured at 30 µM in this thesis vs. *Gonzalez's*[40] thesis.

4.4 Discussion

As was reported in Chapter 2, there is a wide range of values found for the diffusion coefficients of various molecules within bone tissue (figure 2.4). This wide range can be due to many variables. One main reason for the wide range of values found among researchers is the different animal models used in the experiments to measure diffusion. Some researchers used bone tissue from a rat, however rats do not have osteons nor do they have a similar bone microstructure to humans. Another variable is the molecule used to measure diffusion. Fluorescein is most appropriate because it is an amphipathic molecule similar to natural signaling factors diffusing through bone allowing for more accurate measurements. Finally, diffusion across the entire heterogeneous structure should be measured, not just across a single canal. When compared to the value in Figure 2.5, all three of the measured diffusion coefficients in this thesis fall within the range of values previously measured. Since this experiment measured diffusion across the entire bone tissue sample using an amphipathic molecule in an animal model with osteons, it is logical that our measured values are slower than the *Wang et al*[27] value which spotlighted on a single canaliculi, but faster than *Knothe-Tate*[26] value which focused only on the dense tissue between two canaliculi and also used a larger test molecule. The measured diffusion coefficient value using 0.3 μM fluorescein in PBS by *Farrell*[39] of 1.27×10^{-7} cm^2/s is very close to the measured value of this thesis' experimental trials using 0.3 μM fluorescein in PBS which is reported at 1.57×10^{-7} cm^2/s (Figure 4.7).

In order to present a timeframe for the diffusion of fluorescein through canine cortical bone it is necessary to use Einstein's equation to approximate the time (*t*) it takes a specific molecule to diffuse a distance in two dimensions[11]:

$$t \approx \frac{x^2}{2D_{ij}}$$

In this equation *x* is the distance traveled, *t* is the time required, and D_{ij} is the diffusion coefficient. The maximum distance between a Haversian canal and an osteocyte is 100 μm[44]. With this equation it is now possible to calculate the time required for each of the previous researchers' test molecules to diffuse using the diffusion coefficients found in figure 2.4 using 100 μm as the average distance. The fastest time was around 15 seconds through a single canaliculi by *Wang et al*[27] and the slowest being a little over 46 hours by *Knothe-Tate*[26] using a 3000 Da dye through the entire cortical bone. This thesis work used the same marker molecule as Wang's group, and found that it would take roughly 5, 12, and 61 minutes at 0.3, 30, and 300 μM respectively for diffusion in an osteon without loading to occur. The marker used is only 376 Da, roughly the size of Vitamin D (384 Da), and gives a solid baseline for diffusion of small nutrients. It should be pointed out that most proteins and signaling factors that diffuse into bone are much larger, usually greater than 1000 Da.

During this research, it was found that the concentration of fluorescein in PBS affected the diffusion rate in the bone sample. It was observed that as the initial concentration of fluorescein in PBS in the donor chamber increased, the resulting diffusion coefficients decreased. After searching through other literature looking for anything that found a relationship between solute concentration and diffusivity, only a

couple of references were found. The paper referenced in section 2.5 by *Albro et al.*[34] also reported an inverse relationship between concentration and diffusivity using fluorescein-conjugated dextran diffusion in porous agarose hydrogel under loaded conditions. They believe the results are translatable for similar molecular weight solutes in other porous media. However, literature was also found that reported the opposite relationship. *Weinheimer et al.*[41] reported that the diffusion coefficients of both the detergent Triton X-100 and sodium dodecylsulfate in water both increased as the concentration of each solute was increased. Sodium dodecylsulfate increased more significantly than Triton X-100 as a result of aggregation and electrostatic interaction[41]. A table in *Bird et al.*[42] of various diffusivities in the liquid state show both relationships mentioned. The diffusion of chlorobenzene in bromobenzene shows positive relationship of diffusivity with chlorobenzene at both 10ºC and 40ºC. The diffusion of water in *n*-butanol at 30ºC shows inverse relationship of water diffusivity with water concentration. And finally, the diffusion of ethanol in water at 25ºC has no clear trend. As the concentration of ethanol increases, the diffusion coefficient decreases significantly then steadily increases. Another table found in *Bird et al.*[42] shows that as the concentration increases, the diffusion coefficient also increases for toluene in benzene, toluene in carbon tetrachloride, and decane in hexadecane. It should be pointed out that although the same (and opposite) relationship found in this thesis was also reported in other literature, none of it was performed through bone tissue.

The partition coefficient, Φ, of the solutes is the ratio of the available volume to the void volume. The partition coefficient relates the solubility of the solute in the liquid within the pores of a porous material to the solubility of the solute in the bulk phase at

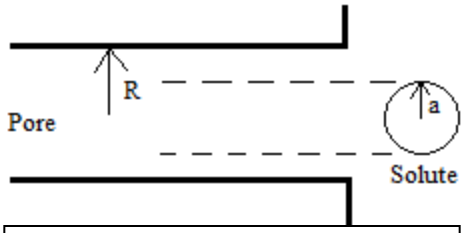

Figure 4.10 Schematic of solute radius (a) vs. pore radius (R).

equilibrium. It was assumed in the diffusion equation in section 3.8 of this thesis (equation 10) that $\Phi=1$. However, even if the liquid in the pores is the same as the liquid in the bulk phase, Φ may not be equal to 1. This is caused by steric hindrance and hydrodynamic friction[11]. How large a factor steric hindrance and hydrodynamic friction are depend on the ratio of a/R, where a is the solute radius and R is the pore radius. If the solute is large, then only a fraction of the pore volume is available to the solute to travel through, meaning $\Phi<1$. But if $a/R << 1$ and the liquid in the pores is the same as the liquid in the bulk phase, then steric hindrance is equal to zero and $\Phi=1$. The solute used in this thesis, fluorescein, has a radius of a=0.00055 µm[43]. If fluorescein were diffusing via a Haversian canal, which have a radius of a=25 µm, the a/R ratio would be 0.00055/25=0.000022 << 1. Another possible route of diffusion for FITC is a Volkmann's canal which has a radius of a=2.5 µm. This a/R ratio would be 0.00055/2.5=0.00022 << 1. Seeing that both these types of pores available to the FITC for diffusion in the bone sample have an a/R ratio << 1, it proves that it was safe to assume that $\Phi=1$ in the overall diffusion equation. However, if $\Phi\neq1$, the resulting diffusion coefficients in this thesis would all change by a factor of $1/\Phi$.

The trials run in this thesis had initial donor concentrations of 0.3, 30, and 300 µM fluorescein (molecular weight of 376 Da) in PBS solution. Average physiological molarities of nutrients similar in size are lower than these initial concentrations. For example, Vitamin D (~400 Da) has a physiological concentration of 0.095 µM. The plot of diffusivity vs. solute concentration using the data in this thesis shows a logarithmic relationship represented by the model equation:

$$D = -2.06E\text{-}8\ln(C) + 1.34E\text{-}7$$

where D is in cm^2/s and C is in µM.

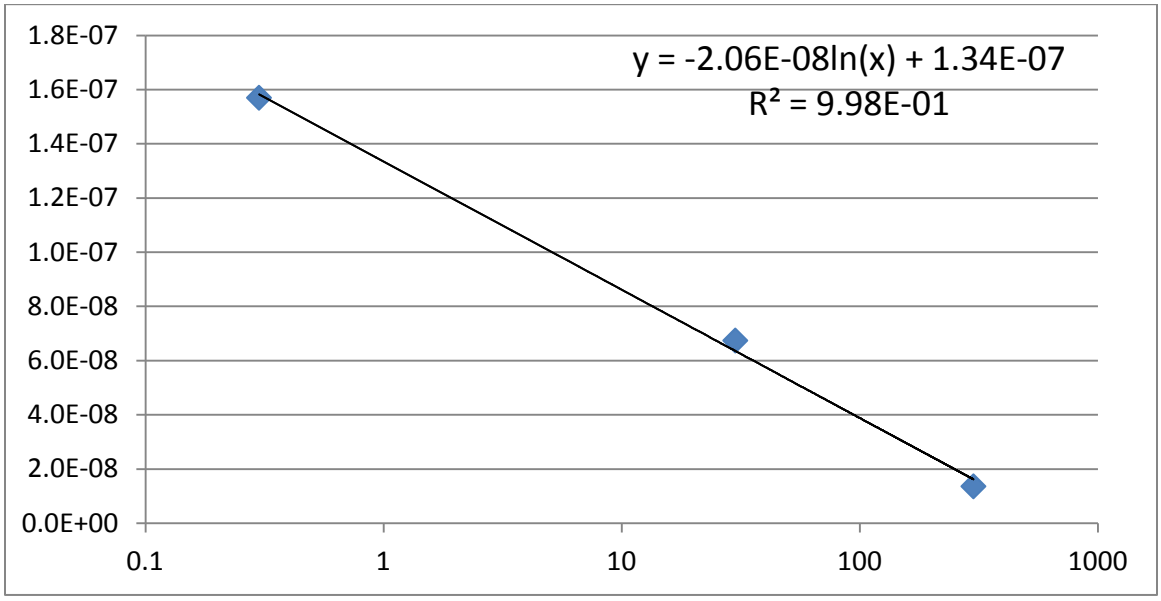

Figure 4.11 Graph of diffusivity vs. solute concentration.

Using this equation, it can be estimated that Vitamin D would have a diffusion coefficient of $1.82x10^{-7}$ cm^2/s at 0.095 µM. However, most of the important signaling molecules diffusing in and out of bone are much larger than a fluorescein molecule (376 Da) such as insulin (2100 Da) and bone morphogenetic protein (14-30 kDa).

Fluorescein can also be degraded and damaged by light so the trials were run in a lab with the lights kept off. However, other students used the lab at times and the lights were occasionally turned on which could have lead to some degradation of the experimental fluorescein.

Bone porosity and connectivity is not uniform throughout its structure so depending on where the bone tissue sample is taken may affect the ability of solutes to diffuse through the sample. In this thesis, only one sample was cut and used from each section and used to measure the diffusion coefficient. Porosity can vary depending on

position on the bone proximally or distally as was concluded in *Farrell*[39]. In his thesis he saw his ability to measure the fluorescent signal from the fluorescein decrease as he moved from the proximal end to the distal end. He hypothesized that was because the proximal end was closest to the epiphyseal plate (growth plate) which may be more porous to allow an influx of nutrients to promote elongation and growth. Although all measurements done in this thesis work were taken from the middle portion of the tibia, the more proximal section 3 showed slower diffusion rates than the more distal section 4. These results are the opposite of what *Farrell* found in his work.

The orthodontic resin used to mount the bone tissue sample did not fully bond to the outer plastic ring or the bone so Krazy Glue was used to seal the plastic-resin and resin-bone interfaces. Some of the Krazy Glue covered the surface of the bone sample reducing the surface area and possible pores available for diffusion leading to a possible small error in the diffusion coefficient measurements. Taking microscope images, montaging them, and putting the montaged image into a MATLAB code to find the area covered by Krazy Glue was attempted but ultimately failed due to montaging problems. This was why the exact surface area available for diffusion was not known, but only an area measured with calipers. Also, it was difficult to cut the exact thickness of the bone sample desired due to the set-up of the low-speed saw. Often times the saw would cut the sample at angle leaving a bone tissue sample of varying thickness across its area, so an average thickness was measured and used in the calculations.

The aim of this thesis was to perform all trials *in vitro* and only measure for diffusion. However, there were several other important modes of transport such as convection, mechanical loading, and gradients such as pressure and electrical that was

absent and/or unaccounted for. These, along with diffusion, can either increase or decrease the rate of transport of crucial molecules needed in the bone. Temperature is another important factor in the transport rates of molecules. The water bath was set at a physiologically relevant 37ºC, however the temperature in the lab room fluctuated depending on the outside season and if the AC/heat was turned on. These changing variables could have led to fluctuations in the water bath temperature, especially in the summer. In hindsight, using a separate temperature monitor kept in the receiver chamber would have been ideal to truly monitor the temperature.

CHAPTER V

CONCLUSIONS AND RECOMMENDATIONS

The diffusion coefficient of a 376 Da fluorescein sodium salt in a canine tibia was measured *in vitro* in PBS at 37°C in a two-chamber diffusion cell. To model the results a quasi-steady state diffusion transport equation was used, focusing in the radial direction through the bone tissue. There was no mechanical loading or external stimuli applied to the system and there was no production or consumption of materials or nutrients by the bone tissue.

5.1 Conclusions

The results from this experiment lead to these conclusions:

- The diffusion coefficients quantified via the transport model for each initial concentration used (0.3, 30, 300 μM) were as follows:
    - At 0.3 μM: $1.57x10^{-7} \pm 3.17x10^{-8}$ cm^2/s
    - At 30 μM: $6.74x10^{-8} \pm 1.00x10^{-8}$ cm^2/s
    - At 300 μM: $1.36x10^{-8} \pm 1.93x10^{-9}$ cm^2/s
- The overall diffusion coefficients (D) decrease as the initial concentration of the donor chamber (C_O) increases.
- In order for diffusion to be measured in the bone tissue sample, there must be some degree of radial connectivity in the bone sample given the conditions and transport model used in this thesis experiment.
- The experimental design can be duplicated while introducing new experimental variables such as mechanical loading or larger solute molecules.

5.2 Recommendations

In order to better understand the diffusivity of solutes in bone tissue the following recommendations should be looked in to for further studies:

- Since fluorescein is on the lower end of the size spectrum for signaling molecules in bone, further research should be performed using larger molecules, such as insulin (2100 Da) to measure diffusion coefficients.
- Additional external stimuli such as mechanical loading and electrical gradients should be introduced and investigated for a more physiologically similar

environment. However, a new equation and experimental set-up would be required.

- A less complicated bone tissue sample mounting procedure that does not involve Krazy Glue should be investigated as to not cause an error in the surface area available for diffusion.
- Build a custom sample holder that is specifically made to hold the bone tissue sample to ensure optimal surface area availability for diffusion and no possibility of leakage between resin-plastic and resin-bone interfaces. Ideally, it should be one that does not need resin, plastic, or Krazy Glue.

REFERENCES

[1] Lian, Jane, Gorski J., and Ott S., Bone structure and function. *ASBMR Education Materials*. N.p., 16 Jan 2004. Web. 22 July 2013.

[2] Moore, Keith L., A. M. R. Agur, and Arthur F. Dalley., *Essential Clinical Anatomy*. Baltimore, MD: Lippincott Williams & Wilkins, 2011. Print.

[3] Dirksen T.R., Marinetti G.V. Lipids of bovine enamel and dentin and human bone. *Calc Tissue Res*. (1970) Volume 6 pg. 1-10.

[4] Pietrazk W.S., Woodell-May J. The composition of human cortical allograft bone derived from FDA/AATB-screened donor. *Journal of Craniofacial Surgery*. (2005) Volume 4 pg. 579-585.

[5] Wang X., Nyman J.S., Dong X., Reyes M., Fundamental biomechanics in bone tissue engineering. Morgan & Claypool publishing. (2010) pg. 15-25.

[6] Martin R.B., Burr D.B., Skeletal tissue mechanics. Springer. (1998) pg. 221-222.

[7] Schlaffler M.B., Burr D.B., Stiffness of compact bone: effects of porosity and density. *Journal of Biomechanics*. (1998) Volume 21-1. Pg. 6-13.

[8] Bilezikian J.P., Raisz L.G., Rodan G.A., Principles of bone biology. Academic Press. (1996) pg.1-10.

[9] Black J., Mattson R., Korostoff E., Haversian osteons: size distribution, internal structure, and orientation. *Journal of Biomedical Material*. (1974) Volume 8 pg. 299-319.

[10] Cooper D., Turinsky A., Sensen C., Hallgrimsson B., Effect of voxel size on 3D micro-CT analysis of cortical bone porosity. *Calcified Tissue International*. (2007) Volume 80 pg. 211-219.

[11] Truskey G.A., Yuan F., Katz D.F., Transport Phenomena in Biological Systems. Pearson Prentice Hall Bioengineering. (2009) Chapters 1 & 7.

[12] Wen D., Cortical Bone Tissue Engineering: Scaffold Design and Cell Selection. Doctoral Dissertation, Cleveland State University. May 2009.

[13] Wen D., Androjna C., Belovich J., Midura R., Lipids and Collagen Matrix Restrict the Hydrolic Permeability Within the Porous Compartent of Adult Cortical Bone. *Annals of Biomedical Engineering*. (2010) Volume 38.

[14] Hollinger J.O., Einhorn T.A., Doll B.A., Sfeir C., Bone Tissue Engineering. CRC Press. (2000) pg. 231-245.

[15] Knothe-Tate M.L., An ex-vivo model to study transport processes and fluid flow in loaded bone. *Journal of Biomechanics*. (1999). Volume 33 pg. 247-254.

[16] Pallua N., Suscheck C.V., Tissue engineering from lab to clinic. Springer. (2011) pg. 140-143.

[17] Li G.P., Bronk J.T., An K.N., Kelly P.J., Permeability of cortical bone of canine tibiae. *Microvascular Res*. (1987) Volume 34 pg. 302-310.

[18] Burg, Karen J.L., Porter, Scott, Kellam, James F., Biomaterial developments for bone tissue engineering. *Biomaterials*. (2000) Volume 4 pg. 433-456.

[19] Meinel L, Karageoriou V., Fajardo-Snyder R.B., Shinde-Patil V., Zichner L., Bone tissue engineering using human mesenchymal stem cells: effect of scaffold material and medium flow. *Annuals of Biomedical Engineering*. (2004) Volume 32 pg. 112-122.

[20] Demirel Y., Nonequilibrium Thermodynamics: Transport and Rate Processes in Physical, Chemical, and Biological Systems. Elsevier. (2007) pg. 357-360.

[21] Dillamen R.M., Roe R.D., Gay D.M., Fluid movement in bone: theoretical and empirical. *Journal of Biomechanics*. (1991) Volume 24 pg. 163-177.

[22] Mishra S., Knothe-Tate M.L., Effect of lacunocanalicular architecture on hydraulic conductance in bone tissue: implications for bone health and evolution. The Anatomical Record. (2003) Volume 273A pg. 752-762.

[23] Carmona R.H., Bone Health and Osteoporosis: A Report of the Surgeon General. Rockville, MD: U.S. Dept. of Health and Human Services, Public Health Service, Office of the Surgeon General. (2004) Print.

[24] SEER Training Modules." *SEER Training: Structure of Bone Tissue*. National Cancer Institute, n.d. Web. 08 Dec. 2013.

[25] Hulbert S.F., Young F.A., Mathews R.S., Potential of ceramic materials as permanently implantable skeletal prostheses. *Journal of Biomaterials Research*. (1970). Volume 4 pg. 433-456.

[26] Patel R.B., O'Leary J.M., Knothe-Tate M.L., Determining the permeability of cortical bone at multiple length scales using fluorescence recovery after photobleaching technique. 51st Annual Meeting of the Orthopedics Research Society. (2007). Paper No. 14.

[27]Wang L., Wang Y., Han Y., In situ measurement of solute transport in the bone lacunar-canalicular system. *PNAS*. (2005). Volume 102 pg. 23.

[28] Knothe-Tate M.L., Steck R., Forwood M.R., In vivo demonstration of load-induced fluid flow in the rat tibia and its potential implications for processes associated with functional adaptation. *Journal of Experimental Biology*. (2000). Volume 203 pg. 2737-2745.

[29] Knothe-Tate M.L., Niederer P., Knothe U., In vivo tracer transport through the lacunocanalucular system of rat bone in an environment devoid of mechanical loading. *Bone*. (1998). Volume 22 pg. 107-117.

[30] Knothe-Tate M.L., Knothe U., Niederer P., Experimental elucidation of mechanical loading induced fluid flow and its potential role in bone metabolism and functional adaptation. *American Journal of the Medical Sciences*. (1998). Volume 316 pg. 189-195.

[31] Lang S.B., Stipanich N.B., Soremi E.A., Diffusion of glucose in stressed and unstressed canine femur in vitro. *Annuals New York Academy of Science*. (1974). Volume 238 pg. 139-148.

[32] Fernandez-Seara M.A., Wehrli S.L., Wehrli F.W., Diffusion of exchangeable water in cortical bone studied by nuclear magnetic resonance. *Biophysical Journal*. (2002). Volume 82 pg. 522-529.

[33] An H.Y., Friedman R.J., Animal models in orthopedic research. CRC Press. (1999). pg. 284.

[34] Albro M.B., Rajan V., Li R., Hung C.T., Characterization of the concentration-dependence of solute diffusivity and partitioning in a model dextran-agarose transport system. *Cellular and Molecular Bioengineering*. (2009). Volume 2 No. 3 pg. 295-305.

[35] Wang Y.L., Taylor D.L., Fluorescent microscopy of living cells in culture. Academic Press. (1989) pg. 130-135.

[36] Periasamy N., Verkma A.S., Analysis of fluorophore diffusion by continuous distributions of diffusion coefficients: application to photobleaching measurements of multicomponent and anomalous diffusion. *Biophysical Journal*. (1998) Volume 75 pg. 557-560.

[37] Landolt-Bornstein. Zahlenwerte und functionen. 6. Auflage, II. Springer-Verlag. (1969) Volume 5 pg 645.

[38] Haberlandt R., Molecules interaction with surfaces and interfaces. Springer. (2004) pg. 130.

[39] Farrell K., One dimensional radial diffusion of small molecules (376 Da) in bone tissue. Master's Thesis. Cleveland State University. December 2011.

[40] Gonzalez M., One dimensional radial diffusion of small molecules (376 Da) in bone tissue under mechanical loading. Master's Thesis. Cleveland State University. Expected May 2014.

[41] Weinheimer R.M., Evans D.F., Cussler E.L., Diffusion in surfactant solutions. *Journal of Colloid and Interface Science.* (1981) Volume 80 Issue 2 pg. 357-368.

[42] Bird B., Stewart W., Lightfoot E., *Transport Phenomena*. New York: J. Wiley, 2002. Print.

[43] Jampol, L. M., "Diagnostic Agents in Ophthalmology: Sodium Fluorescein and Other Dyes." *Handbook of Experimental Pharmacology* 69 (1984): 699-714. Print.

[44] "Osteon," *Encyclopædia Britannica Online* (2009); retrieved 23 June 2009

APPENDICES

APPENDIX A

Set-Ups That Did Not Work

- The first set-up of the diffusion cell bone sample holder involved a plastic ring filled with silicone. A hole about the diameter of a hole-punch was drilled in the middle of the silicone to connect the donor and receiver chambers and allow for fluid interchange. The side facing the donor chamber had an area of silicone cut out that the bone slice would sit in and hold in place. This set-up ultimately failed and was discarded due to leaks and the desire for a larger surface area available for diffusion.

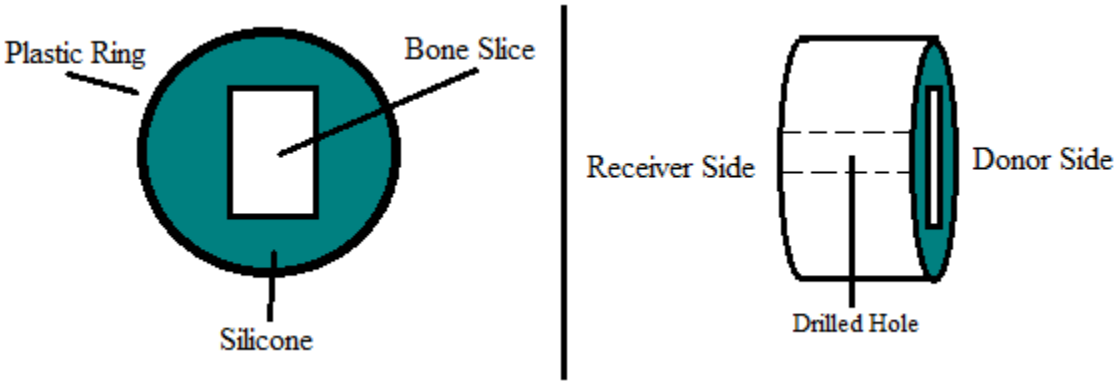

Figure A1. First diffusion cell sample holder set-up.

- The next set up attempted involved two rubber flask stoppers pressed together. This set-up is the where the bone slice in resin was first used. A hole about twice the size of the previous set-up was drilled through the two rubber stoppers. Once the bone-in-resin slice was cut, it was placed in between the two rubber stoppers and Krazy Glued around the edges to hold it in place. The rubber stoppers where

then Krazy Glued together to prevent leakage from between. This set-up ultimately failed and was discarded because the set-up would settle over time and leak from between the stoppers and the glass chambers.

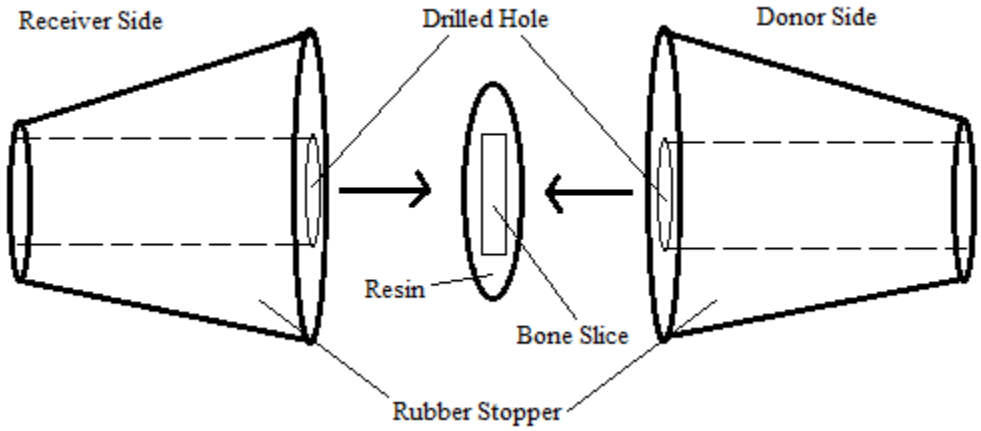

Figure A2. Second diffusion cell sample holder set-up.

- The next set-up attempted involved large metal washers instead of the rubber stoppers with the bone slice in between. This set-up allowed even more surface area available for diffusion and worked pretty well, but was ultimately ditched once the idea of using a filter holder was brought introduced and settled on.

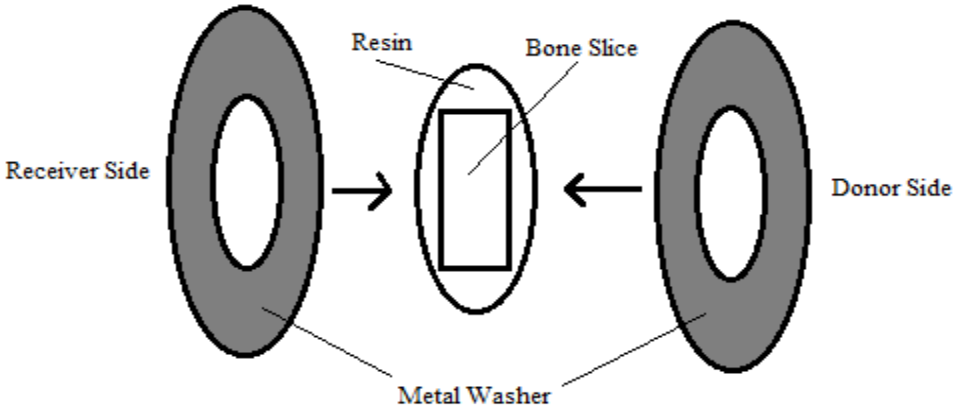

Figure A3. Third diffusion cell sample holder set-up.

APPENDIX B

SEM Images of Bone Section 4 at Varying Magnifications

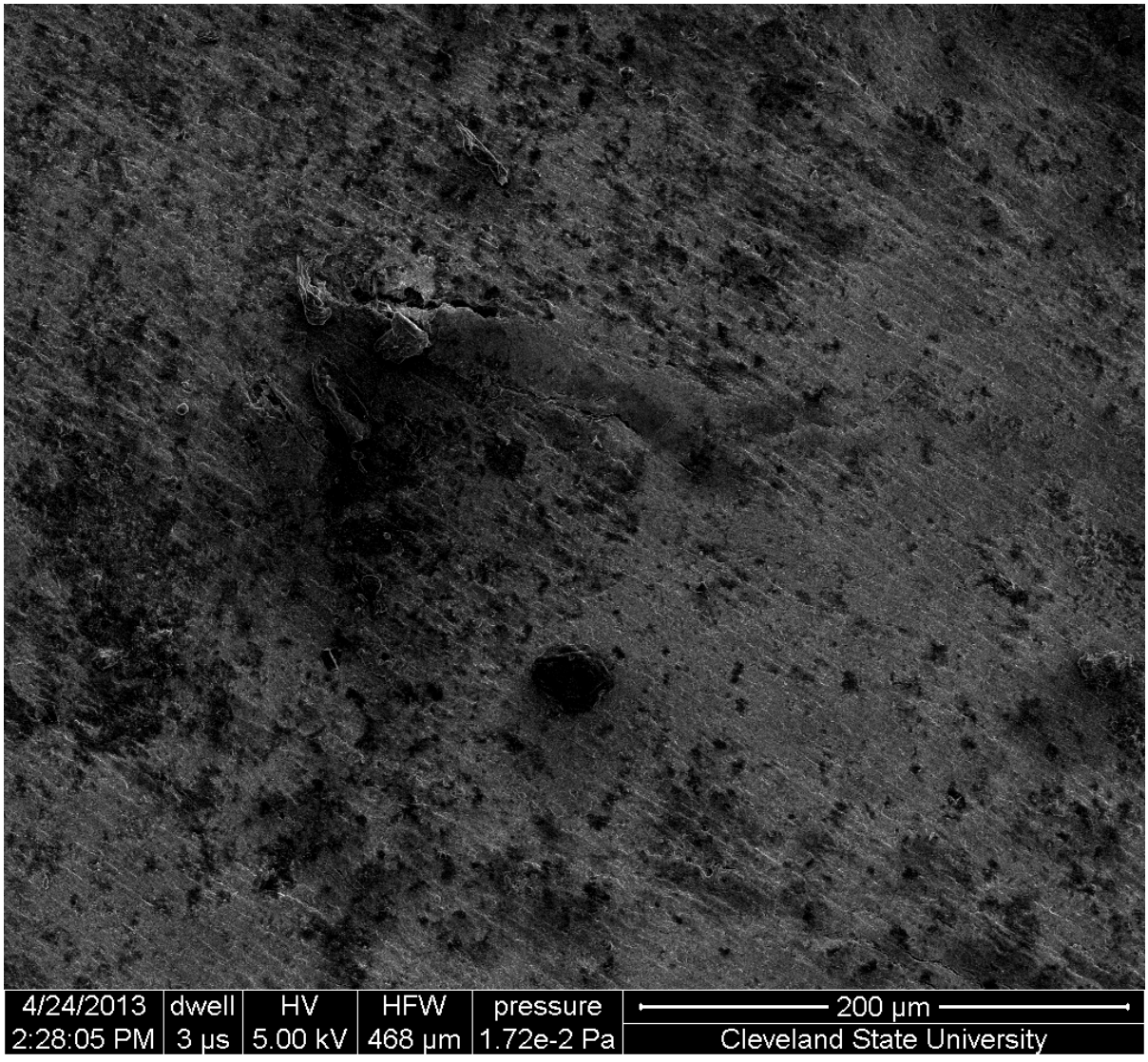

Figure B1. SEM image of bone section 3.

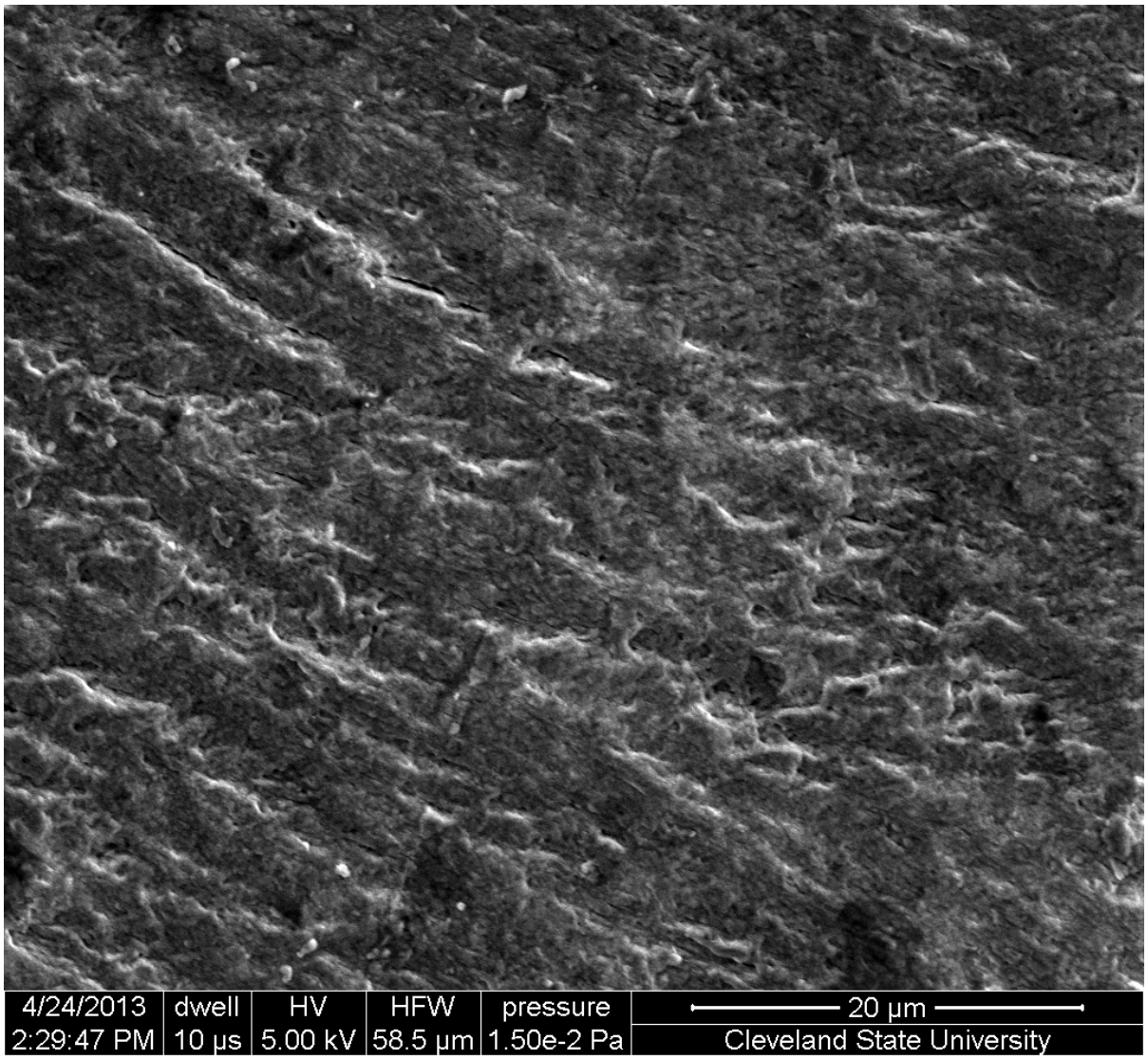

Figure B2. SEM image of bone section 3.

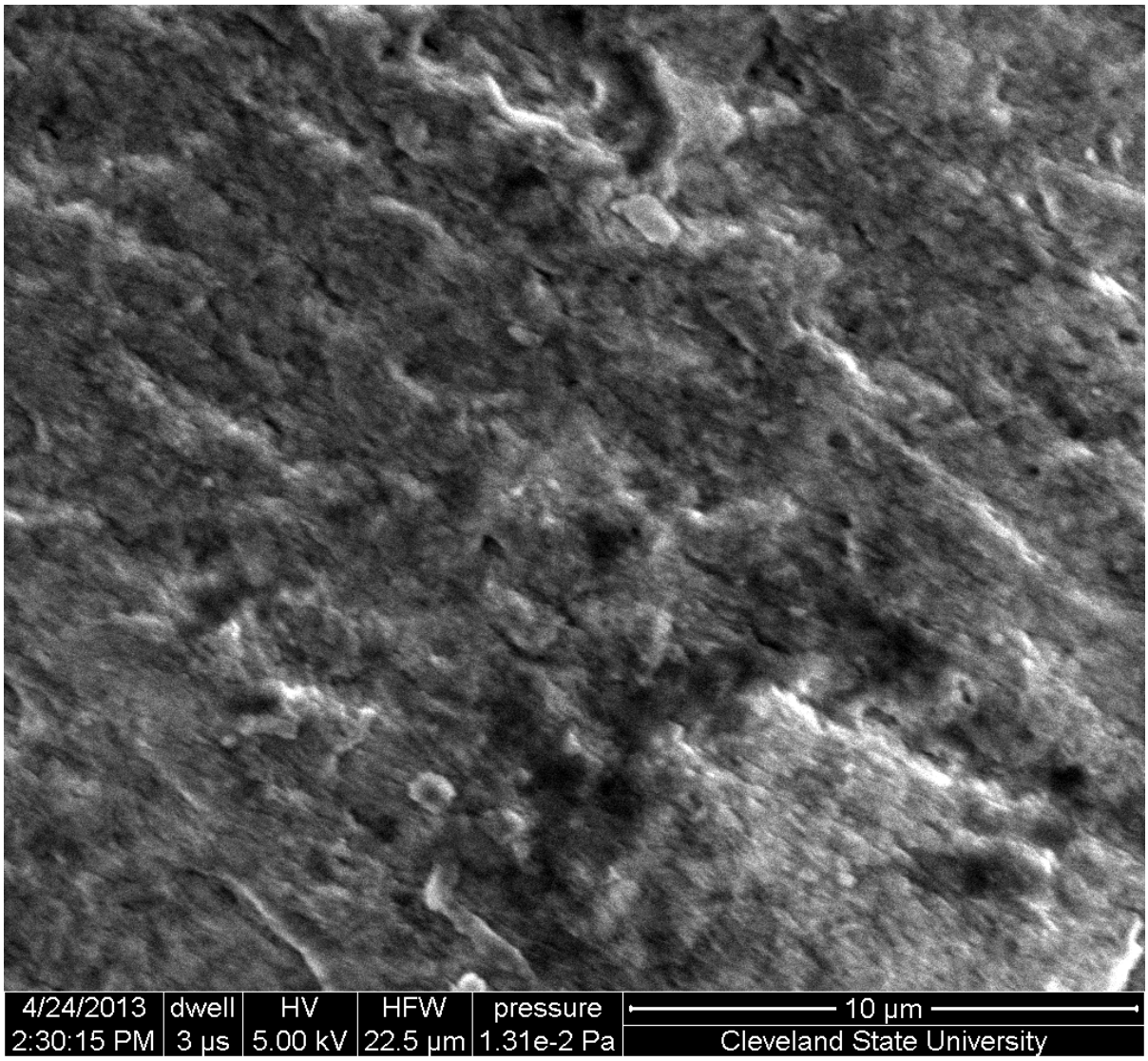

Figure B3. SEM image of bone section 3.

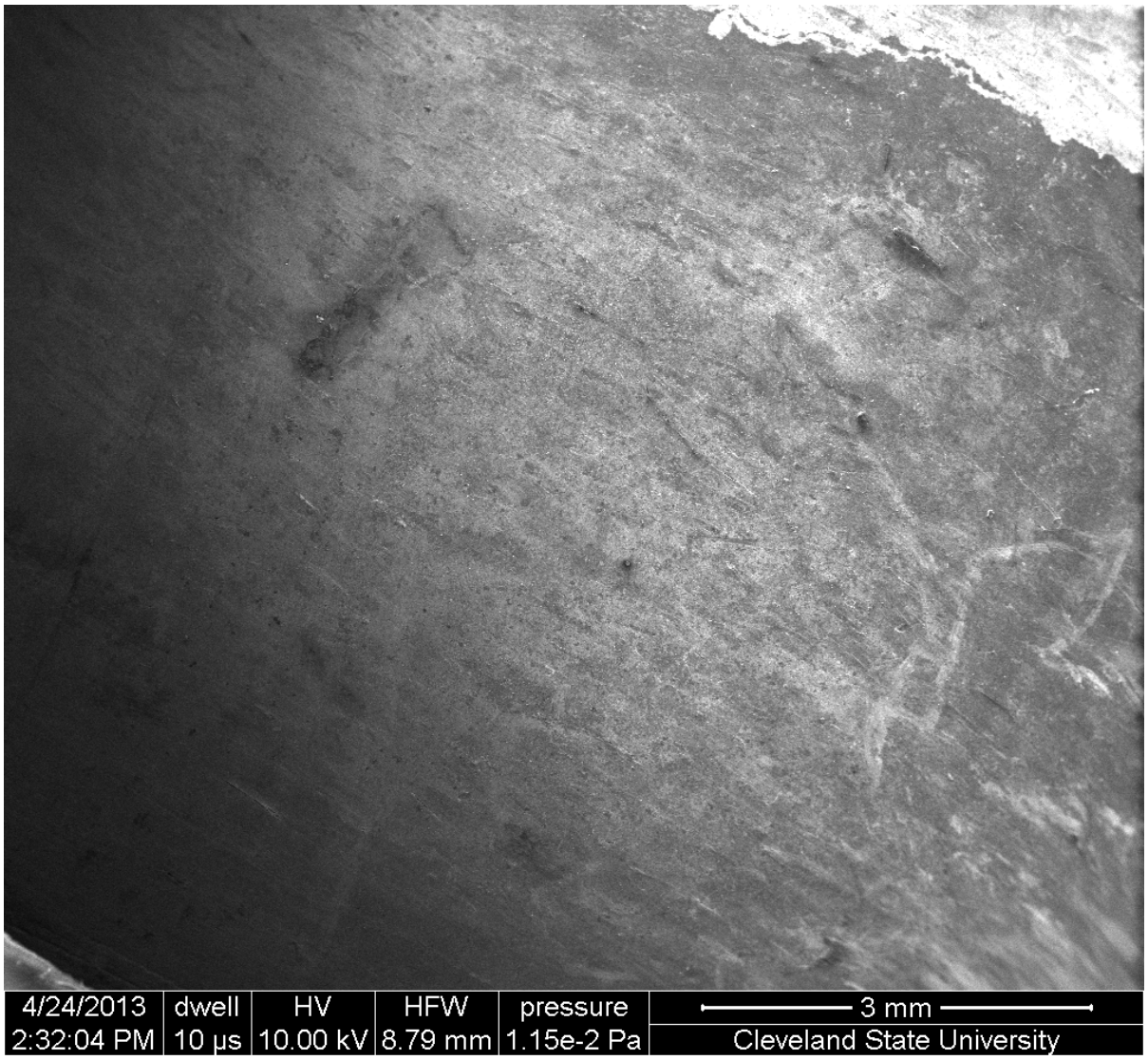

Figure B4. SEM image of bone section 3.

APPENDIX C

Microsoft Excel Procedure to Calculate the Diffusion Coefficient

Once the data results are printed out from the fluorescence spectrophotometer, the data must be entered into various calculations and functions in Microsoft Excel in order for the numerical value of diffusion coefficient to be determined.

1) Open a new spreadsheet. Page 1 is used to reproduce the Calibration Curve in order to add a trendline to get a y=**m**x equation. The slope is important and is used later in step 3. In order to do this, add the Photo Value's to column A and the known Concentrations to column B. Use these numbers to create an x-y plot. Once the plot is created, add a trendline that also gives its equation and R^2 value.
2) Open the next spreadsheet page. Column A and Row 1 are used for headings in order to keep everything in order. A1-A4 are used for Overall Trial #, Section #, Sample #, and Trial # for that bone slice headings. The subsequent columns are used for Time (hours), Photo Value (given by the fluorometer), and Concentration headings.
3) Once the headings are labeled, add the Time and Photo Value data given by the fluorometer in the proper columns. To calculate the concentration for each sample, multiply the Photo Value by the slope (**m** from step 1) of the Calibration Curve. Repeat for all measured samples.
4) Off to the side, create an area to display the Parameter Values. These values include Initial Concentration (C_o), Bone Slice Area (A), Bone Slice Thickness

(L), Cell Volume (V), Slope (m), and B Parameter (B). The B parameter = -2A/VL.

5) Scroll down the page to A20 to begin the next set of calculations. Column A is Time but converted to seconds (multiply the hours column by 3600). Column B is Concentration values (Copy and paste step 3 calculations). Column C is labeled LN(#). The calculation performed in this column is the natural log of the initial donor concentration minus two times the measured receiver chamber concentration, divided by the initial donor concentration. Or, $=LN((C_o-2C_R)/C_o)$.

6) Column C is the left hand side of the overall transport equation:

$$\ln\left(\frac{C_o - 2C_R}{C_o}\right) = -\frac{2A_{Bone}D_{Bone}\Phi t}{VL} = BD_{Bone}t$$

Column C and column A (time (s)) are necessary to perform the LINEST function which is used to help calculate the diffusion coefficient. To perform the LINEST function, select a 2x5 area of cells and click in the function bar. Type: =LINEST(highlight column C values, highlight column A values, FALSE, TRUE) then press ENTER.

Ex: =LINEST(D24:D28,A24:A28,FALSE,TRUE)

7) The 2x5 area will fill with numbers with the first two numbers the most important.

-9.76145E-07	0
9.26978E-08	#N/A
0.965183884	0.083825
110.889324	4
0.779175714	0.028106

Each of the two numbers will be divided by the B parameter to give the overall diffusion coefficient and its standard error for that trial.

8) Example of a finished Excel spreadsheet:

Trial #15	Time (hrs)	Photo Value		[C] 0.3uM, acutal
Section 4	0	11.22		0.007854
Sample 1	28	42.92		0.030044
trial 11	74	61.59		0.043113
	144	86.42		0.060494
	190	97.94		0.068558
Parameter Values				
Co=	0.3	uM		
A=	1.755	cm2		
L=	0.047	cm		
V=	50	cm3		
B=	-1.493617021	cm-2	=-2*A/(V*L)	
calibration slope	0.0007	uM/I		
Time (s)	**[C] 0.3uM, acutal**		**ln()**	
0	0.007854		-0.053780596	
100800	0.030044		-0.223510285	
266400	0.043113		-0.338863092	
518400	0.060494		-0.516329632	
684000	0.068558		-0.610744184	
	LINEST			
	-9.76145E-07	0		**D coeff:**
	9.26978E-08	#N/A		**6.53544E-07**
	0.965183884	0.08382486		**+/-**
	110.889324	4		**-6.20626E-08**
	0.779175714	0.028106428		

Table C1. Example of a completed Excel spreadsheet to calculate the diffusion coefficient.

APPENDIX D

Table of all found diffusion coefficients and their standard error.

Trial #	Diffusion Coefficient	Standard Error
4.1.1. 300 uM	1.22E-08	-1.60E-09
4.1.2. 300uM	1.04E-08	-4.51E-10
4.1.3. 300uM	1.25E-08	-9.41E-10
4.1.5. 30uM	3.50E-07	-3.27E-08
4.1.6. 300uM	1.92E-08	-5.51E-10
4.1.7. 30uM	6.80E-08	-1.34E-09
4.1.8. 30uM	4.97E-08	-1.59E-09
4.1.9. 0.3uM	1.28E-07	-1.17E-08
4.1.10. 30uM	8.44E-08	-3.68E-09
4.1.11. 0.3uM	6.54E-07	-6.21E-08
4.1.12. 0.3uM	1.22E-07	-4.98E-09
4.1.13. 0.3uM	2.20E-07	-2.39E-08
3.1.3. 30uM	1.31E-08	-2.85E-10
3.1.4. 30uM	1.75E-08	-1.83E-09
3.1.5. 30uM	2.90E-08	-4.40E-09

Table D1. All found diffusion coefficients and their standard error.

APPENDIX E

Concentration Log Plots

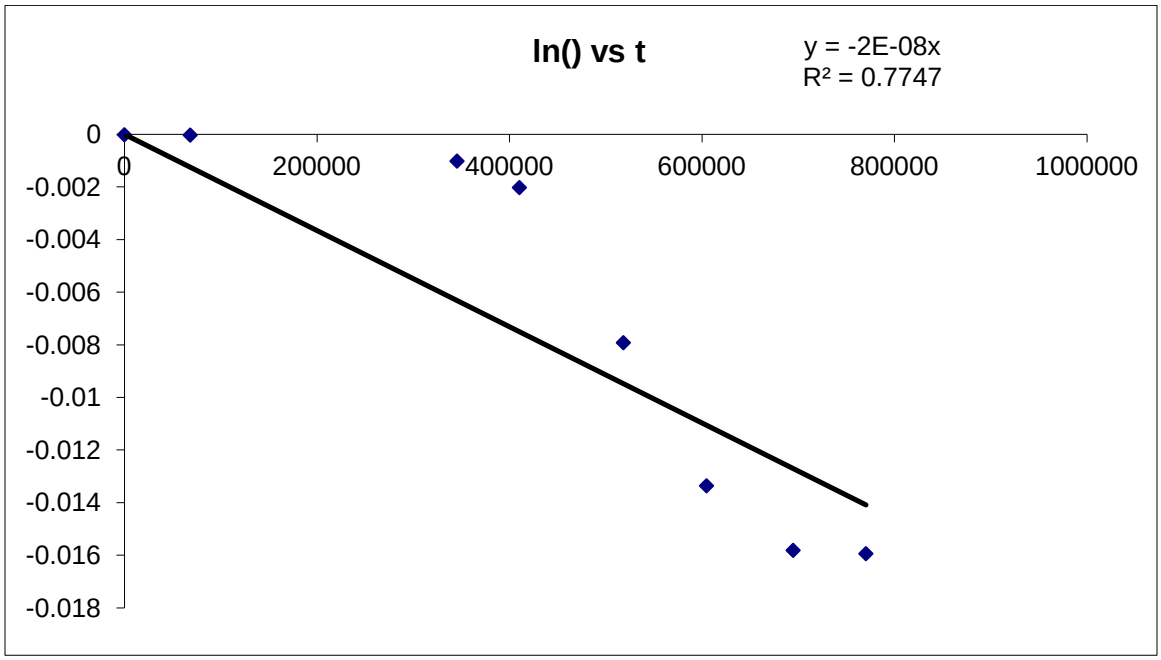

Figure E1. Trial 4.1.1 concentration vs. time log plot.

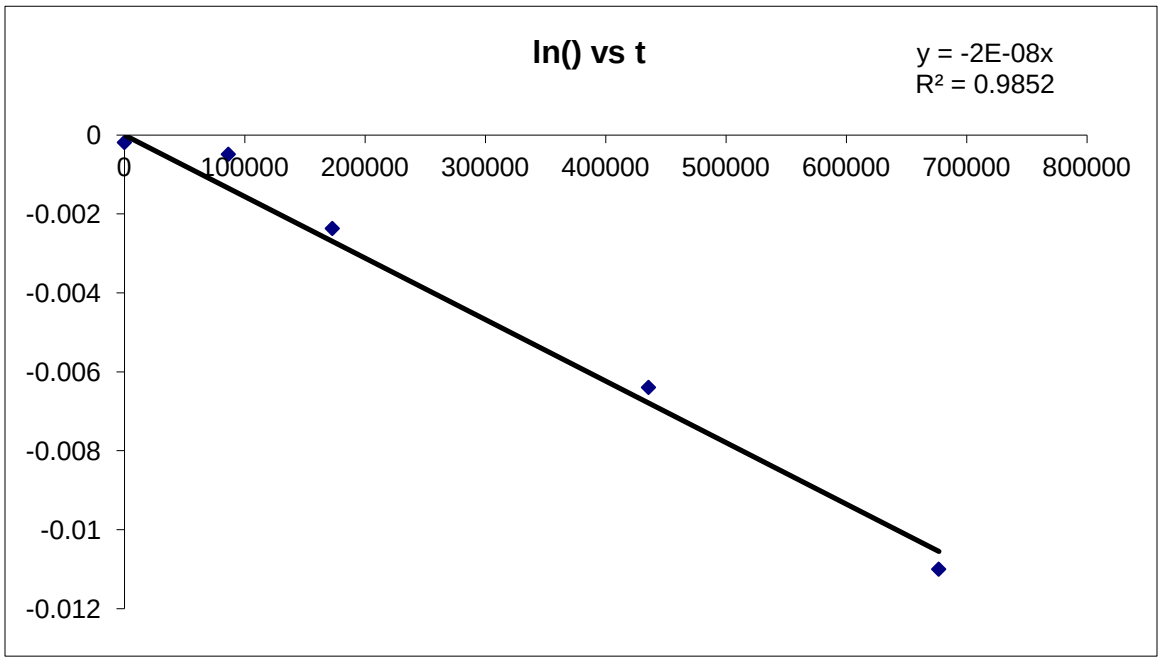

Figure E2. Trial 4.1.2 concentration vs. time log plot

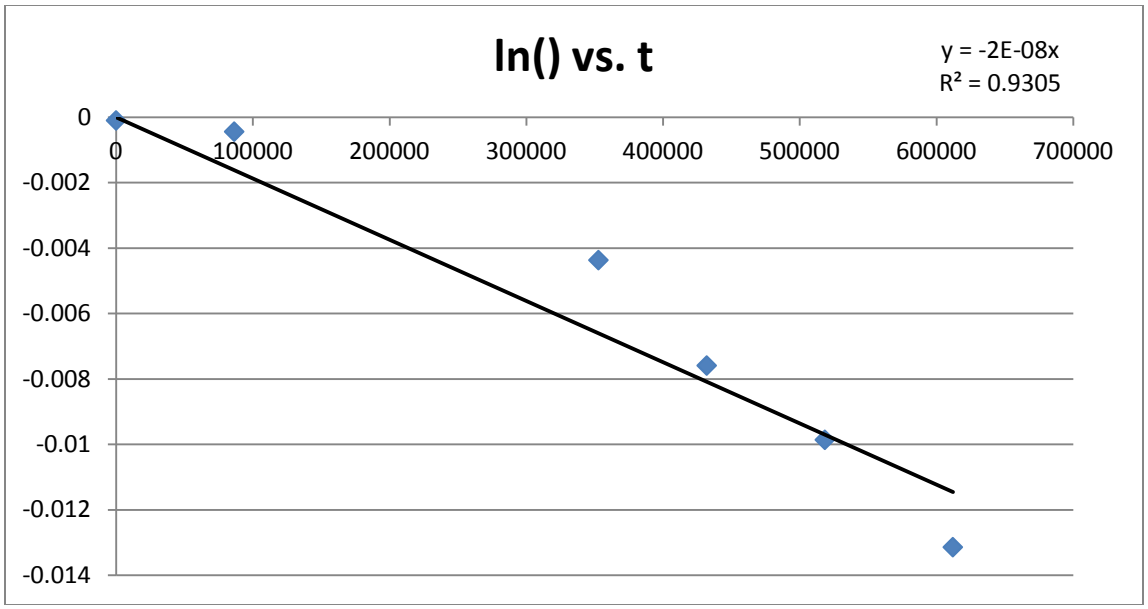

Figure E3. Trial 4.1.3 concentration vs. time log plot.

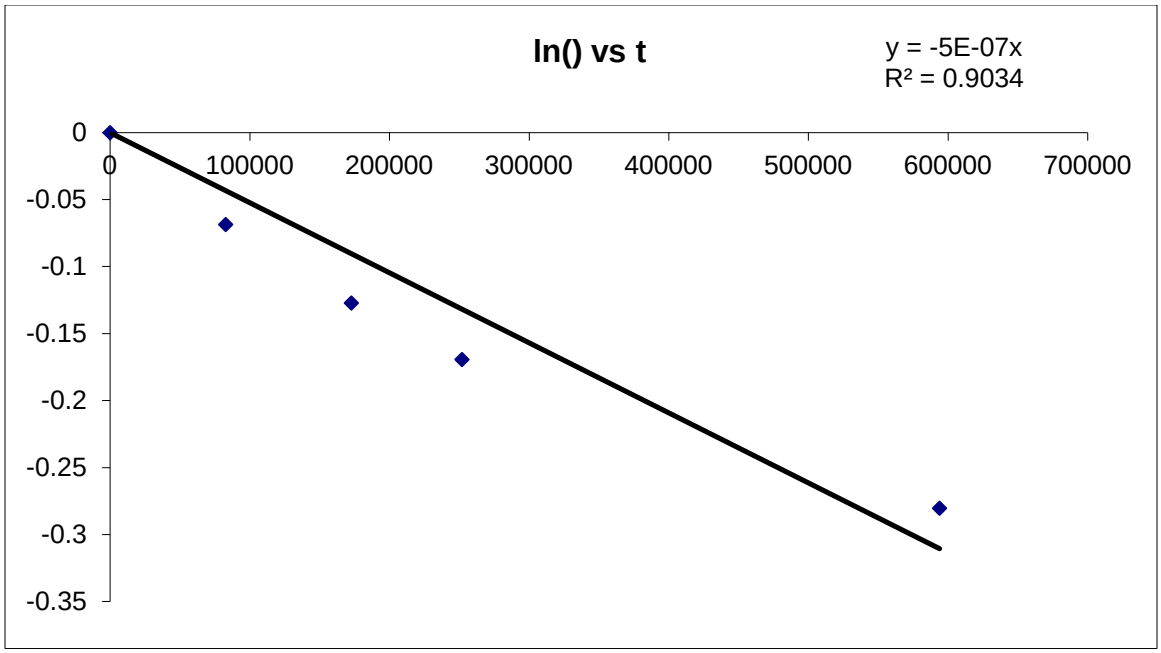

Figure E4. Trial 4.1.5 concentration vs. time log plot.

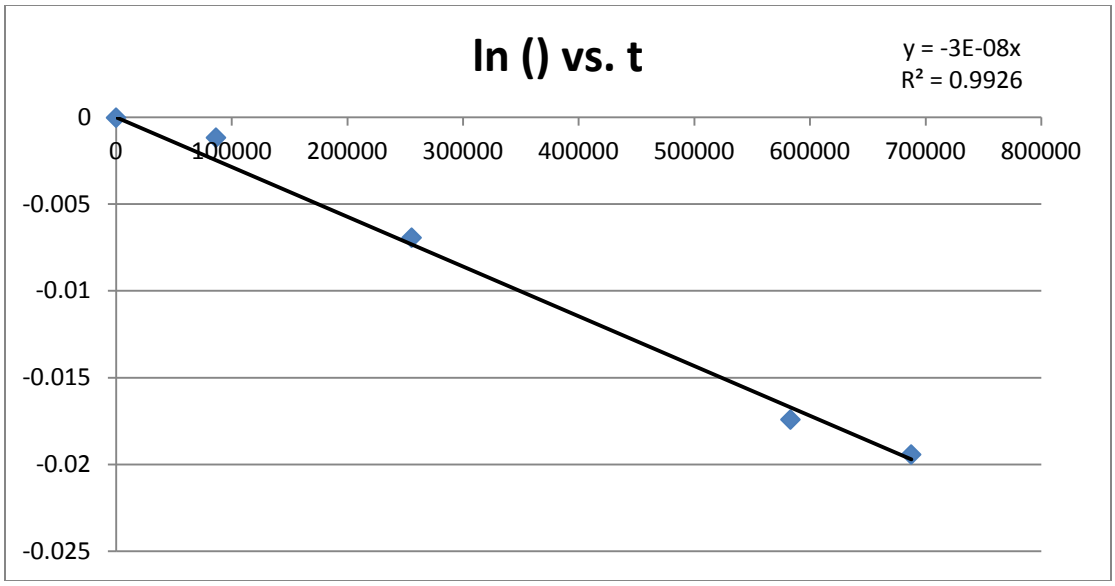

Figure E5. Trial 4.1.6 concentration vs. time log plot.

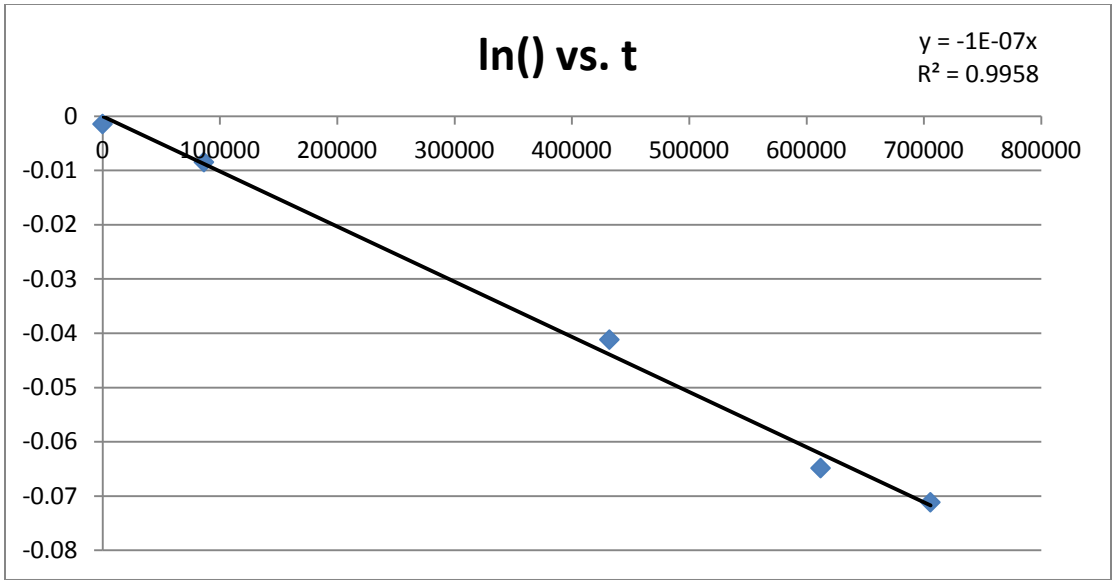

Figure E6. Trial 4.1.7 concentration vs. time log plot.

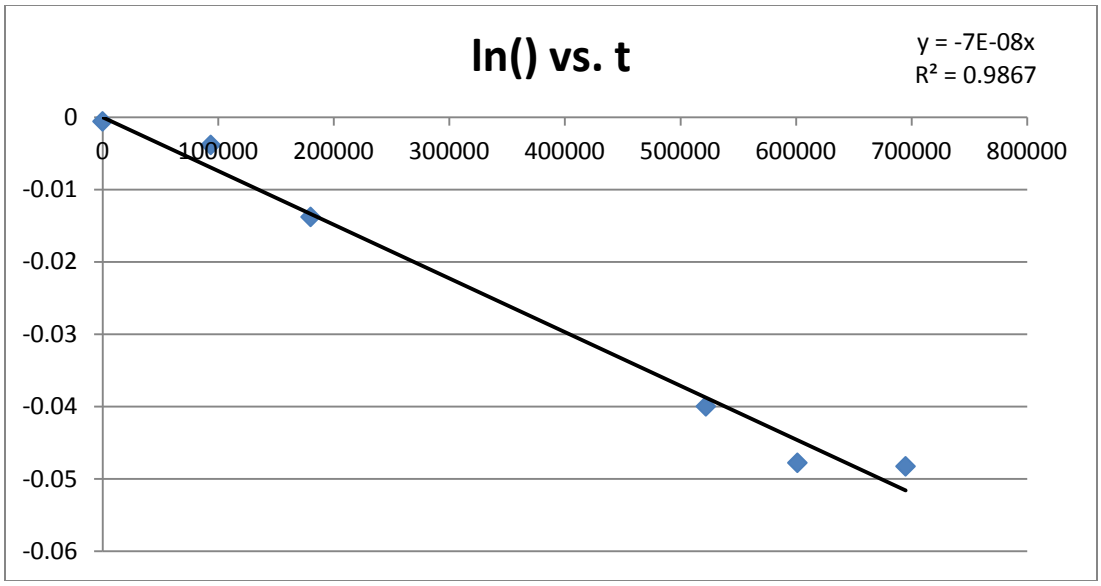

Figure E7. Trial 4.1.8 concentration vs. time log plot.

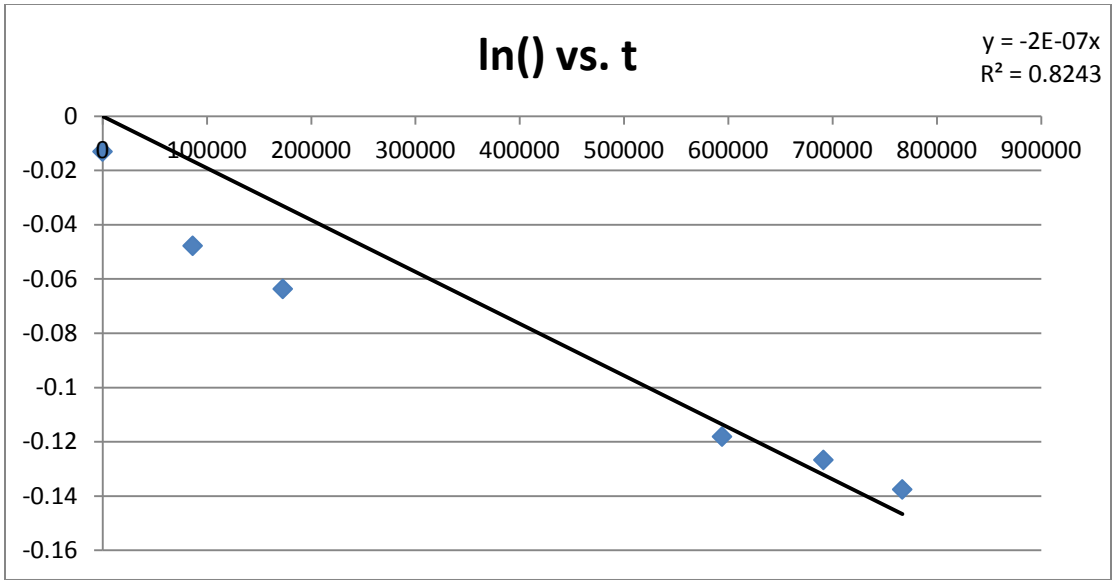

Figure E8. Trial 4.1.9 concentration vs. time log plot.

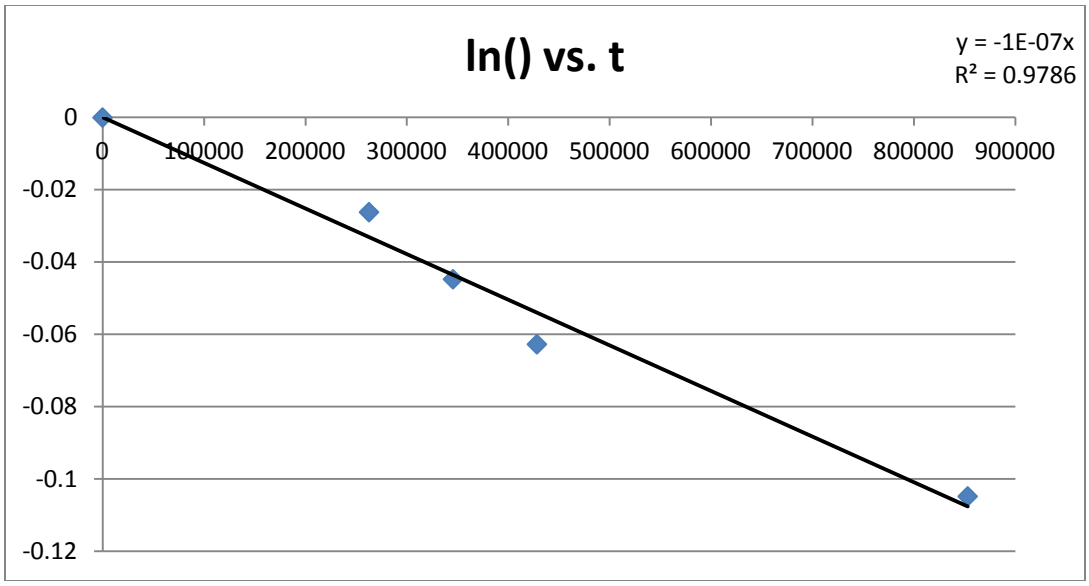

Figure E9. Trial 4.1.10 concentration vs. time log plot.

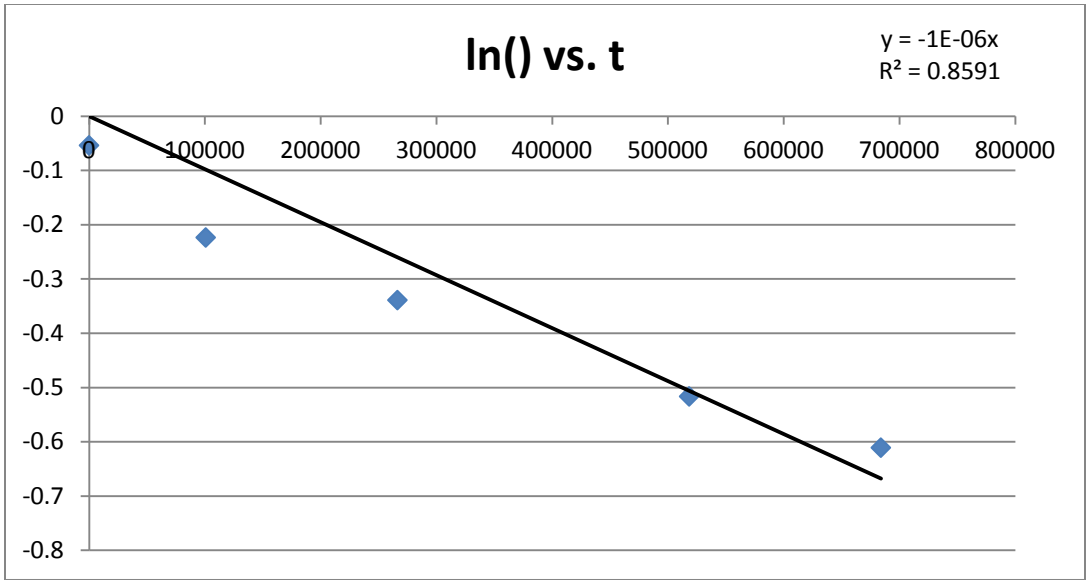

Figure E10. Trial 4.1.11 concentration vs. time log plot.

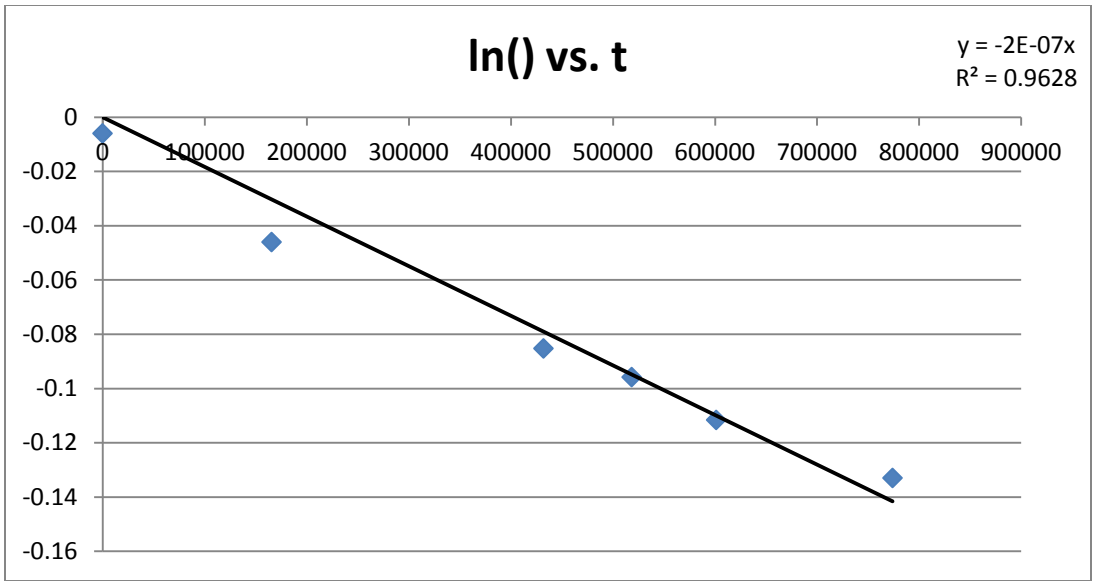

Figure E11. Trial 4.1.12 concentration vs. time log plot.

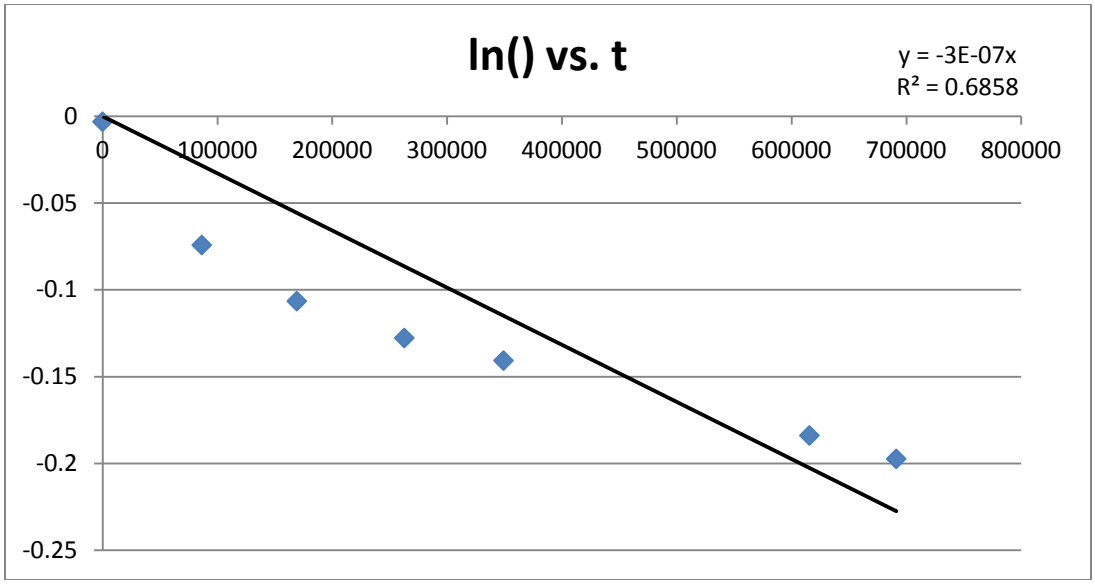

Figure E12. Trial 4.1.13 concentration vs. time log plot.

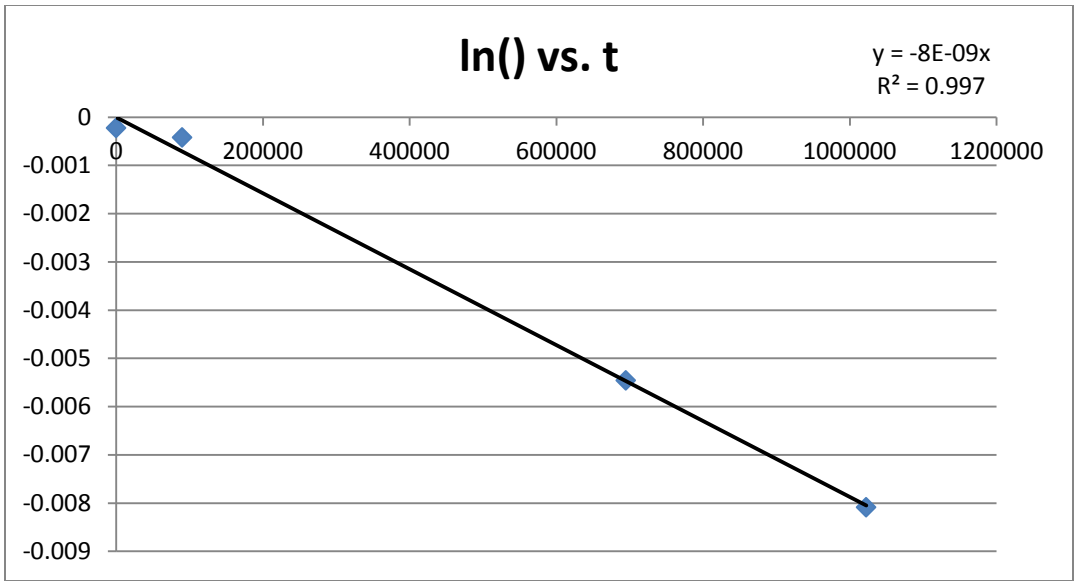

Figure E13. Trial 3.1.3 concentration vs. time log plot.

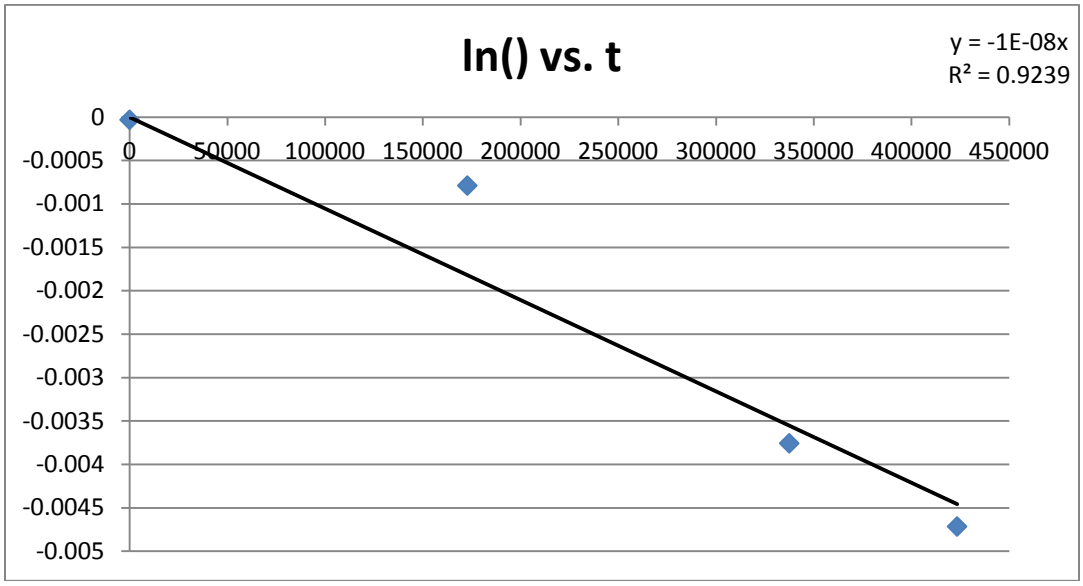

Figure E14. Trial 3.1.4 concentration vs. time log plot.

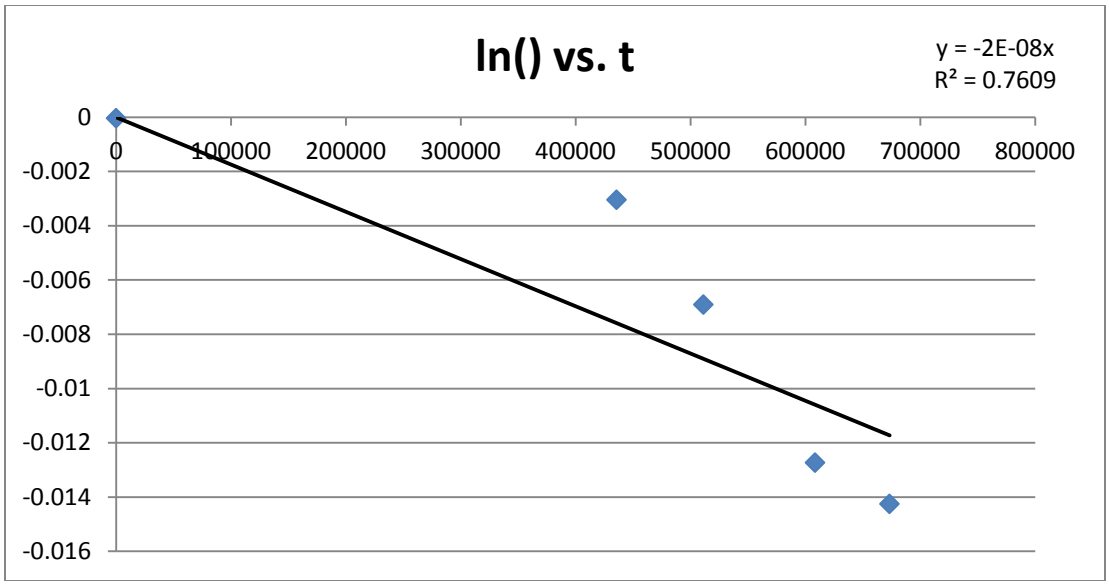

Figure E15. Trial 3.1.5 concentration vs. time log plot.